DECEMBER 18, 2020

STRUCTURE AND FUNCTION OF ELASTIC FIBRES IN HUMAN LUMBAR INTERVERTEBRAL DISCS

Submitted to the College of Science and Engineering in partial fulfilment of the requirements for the degree of Master of Engineering (Biomedical) at Flinders University, Adelaide, Australia

SALINDI HERATH
SUPERVISORS: ASSOCIATE PROFESSOR JOHN COSTI AND DR. JAVAD TAVAKOLI
Flinders University

Declaration

I, H.M. Salindi P. Herath, declare that the work presented in this thesis is my own unless otherwise referenced.

Executive Summary

The structure and function of elastic fibres are poorly understood in human intervertebral discs. It is hypothesized the elastic fibres play a role in the structural integrity of the disc by holding adjacent lamellae together. Previous research found that degenerated discs or discs that were susceptible to herniation had differences in elastic fibre structure and organization compared to healthy discs. Therefore, understanding the structure and function of elastic fibres is necessary for elucidating mechanisms of herniation and disc degeneration. The aim of this thesis was to visualise the ultrastructure of elastic fibres and understand their functional role in human intervertebral discs.

A partial alkali digestion protocol was developed for isolation of elastic fibres in sheep intervertebral discs that was firstly replicated in this project and then optimised for visualisation of elastic fibres in human intervertebral discs. Visualisation was performed by scanning electron microscopy in order to obtain high resolution images that can be quantitatively analysed. During the optimization process of the partial alkali digestion protocol, elastic fibres were found in the lamellae and the ILM region that support the hypothesis on the functional role of elastic fibres in the disc. Further experimentation is required to create a digestion protocol that can be used irrespective of disc region, level, or degeneration. An optimal alkali digestion protocol can be used to visualize differences in elastic fibres in different regions of a disc or discs of varying levels of degeneration. Micromechanical tests can also be conducted on a lamellar unit containing isolated elastic fibres between two lamellae to understand the mechanical contribution of elastic fibres in the disc.

Acknowledgements

I would like to thank my supervisors Associate Professor John Costi and Dr. Javad Tavakoli who assisted me in designing the experiments that were conducted, analysing results, and writing my thesis.

I would also like to acknowledge the assistance of Mr. Michael Russo whose help was tremendous in isolating intervertebral discs from both sheep and human samples. I would also like to acknowledge the assistance of Mr. Alex Sibley who trained me on the scanning electron microscope and Ms. Pat Vilimas for training me on the cryostat microtome.

Table of Contents

Introduction

Back pain is experienced by 16% of Australians irrespective of region according to the National Health Survey conducted in the years 2017 to 2018 (ABS, 2019). Back pain was reported second only to stroke, heart, and vascular disease therefore making it the highest non-fatal chronic illness experienced by Australians. Disc degeneration, the natural aging of the disc, and microstructural changes has been found to be linked with lower back pain and herniation, leakage of nuclear material out of the disc (Tavakoli et al., 2016, Schollum et al., 2008). However, the relationship between microstructural changes and macrolevel changes has not been fully investigated.

Five vertebrae, labelled L1 through L5 from top to bottom, make up the lumbar spine. As the name suggests, the intervertebral disc is located between two vertebrae and is named after the two vertebrae that surround it (Bogduk, 2012). Three components make up intervertebral discs: the annulus fibrosus (AF), the nucleus pulposus (NP), and the vertebral endplates (VEP). The AF surrounds the NP circumferentially while the VEP covers the entire NP and most of the AF inferiorly and superiorly as seen in Figure 1.

Figure 1. Components of the intervertebral disc. Left: transverse section of disc showing the AF and NP. Right: coronal section of disc showing VEP. Image shows VEP attached to the edges of the disc, but the VEP is not attached on the periphery of the disc. (Bogduk, 2012)

Functionally, the intervertebral discs bear load and provide flexibility to the spine. Specifically, the AF and NP bear load and transmit it to the VEP where this load is then passed to the vertebral bodies. Since the VEP is not attached to the AF at the periphery of the disc, when the disc is under compression such as during standing, the vertebral bodies move closer together and the AF bulges radially. This radial bulging is not, however, a permanent deformation as the disc returns to its original shape when the disc is not under compression such as in a supine posture. Radial bulging, however, has been associated with annular tears (Figure 2) that accumulate as we age and can lead to herniation (Vernon-Roberts et al., 2007).

One type of annular tear that is common in people of all ages are concentric tears which is the delamination of the lamellar sheets in the AF.

Image removed due to copyright restriction.

Figure 2. Concentric annular tear. Annular tears occur naturally from daily activities. (Bogduk, 2012)

Collagen, water, and extracellular matrix (ECM) make up the NP. Different concentrations of the same components of the NP along with elastic fibres (EF) make up the AF while the VEP is primarily made of hyaline cartilage. In the NP, the collagen fibres are irregularly arranged, but in the AF, they are highly organized as concentric lamellar sheets, a distinguishable feature of the AF (Bogduk, 2012). Each lamellar sheet is made up of collagen fibres arranged at 60° from the vertical axis in alternating directions between adjacent lamellar sheets (Figure 3). Alternating organization of the collagen fibres allows for bidirectional loading of the disc since collagen is the load bearing component. ECM is a proteoglycan-rich gel that includes connective tissue cells as well (Tavakoli et al., 2016).

Image removed due to copyright restriction.

Figure 3. Lamellar sheets of the AF. Angle θ is 60° showing the direction of the collagen fibres alternating between adjacent lamellar sheets. (Bogduk, 2012)

Bundles of elastin protein surrounded by microfibrils make up EF and they exist all around the AF. Originally observed by light microscope and found in the lamellae and between lamellar sheets to be irregularly distributed, recent investigations using scanning electron microscopy (SEM) have found EF in sheep samples to be highly organized (Tavakoli et al., 2017). In the

space between the lamellar sheets or the interlamellar matrix (ILM), EF were found to form a dense and complex network consisting of large fibres interconnected by smaller fibres that merge into the lamellae and run parallel to the collagen fibres. Function of EF in the disc is poorly understood, however, it is hypothesized from their ultrastructure that they play a role in maintaining the structural integrity of the disc. Specifically, EF are hypothesized in assisting the AF in returning to its original shape following deformation during compression, bending, or shear loading. Failure of the AF to return to its original shape can lead to annular tears during subsequent loading cycles.

One of the macrolevel characteristics of disc degeneration is accumulation of annular tears. Annular tears are thought to act as a pathway for nuclear material to leak out of the NP leading to herniation. Degenerated discs and discs susceptible to herniation have displayed microstructural changes such as changes in the organization and density of EF (Yu et al., 2005). Ultrastructure of EF in humans has not been described in detail and the functional role of EF has not been investigated either. It is evident, however, that there is a connection between EF and disc degeneration that will be described in detail in the literature review. Briefly, changes in the EF organization within discs can be seen in degenerated discs and ultrastructure of EF in the ILM indicates a function in preventing annular tears. However, the mechanisms by which disc degeneration occurs and the role of EF in this process is not fully understood. Due to microscopy advancements, sheep EF structure and function have been investigated in detail, but clinical relevance of EF structure and function can only be considered in human samples. In sheep studies, EF were hypothesized to play a role in maintaining the structural integrity of the intervertebral discs and allow the disc to return to its original shape after deformation.

An alkali partial digestion protocol using sodium hydroxide (NaOH) was developed by Dr. Javad Tavakoli that has been used to visualize EF in sheep samples using SEM (Tavakoli and Costi, 2018a, Tavakoli and Costi, 2017). In this procedure, the samples are sonicated in NaOH followed by heat treatment in hot water (70°C). This procedure has shown success for visualisation of EF in human samples but has not been used extensively and therefore it needs to be optimised for human samples (Tavakoli and Costi, 2018a). Using this partial digestion protocol as opposed to other methods is advantageous since this method allows for clear visualisation of EF by removal of components that obscure the network and SEM images are

of high resolution allowing for quantitative analysis of the EF network. The aim of this project was to optimise the partial alkali digestion protocol for visualisation of EF in human samples.

Before attempting to optimise the partial digestion protocol for use on human samples, the original method was replicated, and EF were visualised in sheep samples in order to learn the procedure. Once EF in sheep samples were successfully visualised, optimization occurred in a series of steps that relied on the results of the previous step. In developing the original partial digestion protocol for use in sheep samples, increasing sonication time showed better visualisation of the EF network (Tavakoli and Costi, 2018a, Tavakoli and Costi, 2017). Therefore, varying sonication time was the first experiment in the optimization process. Next steps in optimization included soaking the samples in NaOH overnight, increasing the molarity of the NaOH, and varying sonication time in a higher concentrated NaOH solution.

In the literature review, the relevance of EF research will be outlined along with its connection to disc degeneration and back pain. Then for each experiment using both sheep samples and human samples, the partial digestion protocol will be described in detail along with the results that were obtained. Finally, the overall results of the project will be discussed along with future directions for this work. This project aims to create an optimised alkali digestion protocol for visualisation of EF in human samples that can be used to investigate the structure and function of EF in humans to understand mechanisms of disc degeneration.

Literature Review

Disruption of the ECM and accumulation of concentric tears are characteristics of disc degeneration, herniation, and back pain (Gregory et al., 2014, Gregory et al., 2012, Fazzalari et al., 2001). Herniation (leakage of nuclear material outside of the disc) has been hypothesized to occur because of microstructural changes that occur during disc degeneration (Veres et al., 2010). Loading of the disc during daily activities was found to create concentric tears in the annulus that accumulate throughout our lifetimes as seen in cadavers of varying ages (Vernon-Roberts et al., 2007). Concentric tears create a pathway for herniation to occur (Veres et al., 2009). When compression was simulated by increasing hydrostatic pressure in the NP, annular tears were found to form primarily in the posterior annulus fibrosus (Veres et al., 2008). Outer posterior regions of the AF also exhibit partial or incomplete lamellae (Bogduk, 2012).

Microstructural changes caused by aging lead to annular tears that create a pathway for nuclear material to leak, which results in mechanical property changes in the disc. Annular tears were found to increase the stiffness of the disc and shift pressure distribution causing an increase in pressure in the AF compared to discs without tears. As a result of these changes, subsequent loading can lead to further tears in the disc (Lee et al., 2004, Fazzalari et al., 2001). Delamination of the annulus fibrosus, accumulation of concentric tears, and herniation are all associated with local failure of the ILM (Veres et al., 2008, Gregory et al., 2014, Gregory et al., 2012). Microstructural changes that lead to failure of the ILM and delamination creates a pathway for nuclear material to leak out during loading of the disc (Tavakoli et al., 2018). Interestingly, outer posterior regions of the disc were found to be most susceptible to failure in the presence of pressurization and could likely be caused by the lack of complete lamellae in this region (Veres et al., 2008). It is important therefore to understand the mechanisms by which annular tears and degeneration occur at a microstructural level to prevent herniation and pain.

The ILM is composed of ECM, EF, and cells. The ECM consists of water, proteoglycans, and lipids and their role is to maintain hydration of the disc and provide lubrication between the lamellae (Iatridis et al., 2007). One of the main components of the ILM are EF which are made of an elastin core and microfibrils (Smith and Fazzalari, 2009) and they are thought to play a role in maintaining the structural integrity of the interlamellar matrix (Tavakoli et al., 2018).

Higher concentrations of EF were found in the outer annulus compared to the inner annulus (Smith and Fazzalari, 2006). Within the ILM, EF were found to create a dense and complex network (Yu et al., 2007, Smith and Fazzalari, 2006) with thicker EF interconnected by thinner EF (Tavakoli and Costi, 2018a). Thicker EF were found to merge into the lamellae at the boundary between the ILM and the lamellae, and orient parallel to the collagen bundles within the lamellae. At the partition boundary, the region between collagen bundles within the lamellae, the EF were found to be of various sizes and create an organized network merging in parallel or penetrating the collagen bundles (Tavakoli and Costi, 2018d). Based on the ultrastructure of EF, they have been hypothesized to play a role in maintaining the structural integrity of the disc by holding lamellae together to restrict lamellar separation and radial bulging (Smith et al., 2008, Tavakoli et al., 2017).

Ultrastructure of EF in the ILM suggests orthotropic mechanical properties which was consistent with micromechanical tests conducted on the EF network in sheep ILM samples with other constituents removed (Tavakoli and Costi, 2018c). In mechanical tests that were conducted on in-tact ILM samples, however, no direction-based differences in failure mechanisms were found indicating that the ECM likely acts as a structural scaffold contributing to the isotropic mechanical properties of the in-tact ILM (Tavakoli and Costi, 2018b). Mechanical tests conducted on AF samples that were enzymatically treated to remove EF found that linear and tensile moduli decreased by 90% in the radial direction and extensibility increased by 431% (Smith et al., 2008). In bovine AF samples that were subject to pre-herniation and herniation by macroscopic compression found that compared to non-herniated AF samples, the ILM was the primary location of failure (Tavakoli et al., 2018). Since EF are the major component of the ILM, their role in disc degeneration and maintaining connectivity between lamellae is evident.

The structure and function of EF in human discs are poorly understood. However, differences in diseased discs versus healthy discs showed evidence of the clinical relevance of EF. In discs that were more prone to disc degeneration, sparse and disrupted EF were found (Yu et al., 2005) and the ILM was found to be weaker in herniated discs compared to non-herniated discs (Tavakoli et al., 2018). Metalloproteinases, a proteolytic enzyme associated with degradation of major ECM elements, was found to be up-regulated in degenerated discs (Bachmeier et al., 2009, Crean et al., 1997). Degradation of elastin by metalloproteinases

leads to the release of elastin peptides into the ECM that initiates biological pathways that may lead to increases in degeneration (Mecham et al., 1997). Elastin peptides bind to calcium channels in the cell membrane which elevates calcium levels in the disc that can be related to the calcification of the VEP that occurs in disc degeneration (Grant et al., 2016, Faury et al., 1998). Furthermore, elastin peptides have been shown to up-regulate metalloproteinases and cause cell proliferation (Jung et al., 1998, Brassart et al., 2001) which can change the density and structure of the ECM leading to changes in the mechanical properties of the disc. Structure and function of EF have clinical relevance in herniation and disc degeneration.

Location-based variations in the ultrastructure of EF have been visualised in different regions of the disc due to variation in the loading requirements in these regions (Yu et al., 2002, Yu, 2002, Tavakoli et al., 2016). In older studies that visualised the elastic fibre network in the AF, light microscopy has been used in conjunction with conventional histological orcein staining and immunostaining. Orcein staining allowed visualisation of the presence of the EF network, however, ultrastructural details were obscured by ECM and collagen (Yu et al., 2002, Tavakoli and Costi, 2018a). Hyaluronidase in conjunction with collagenase have been used as pre-treatments prior to dual immunostaining with elastin and fibrillin antibody and found that EF were denser in the ILM compared to any other region in the AF (Yu et al., 2007). Immunostaining with just elastin has also shown success in comparing density and orientation of EF in the different areas of the disc (Yu et al., 2002). In the lamellae, EF were parallel to collagen fibres with finer fibres found perpendicular to the collagen fibres, but EF did not appear to have a regular organization (Yu et al., 2002). Treatment of the discs to remove components that surround the EF network was necessary for ultrastructural visualisation of the EF network. However, scanning electron microscopy (SEM) allows for a higher magnification and resolution, therefore providing a higher level of detail compared to light microscopy (Tavakoli and Costi, 2018a).

Older methods provided insight into the general distribution of EF, but they did not provide the resolution required to visualise the fine-scale ultrastructure of EF (Tavakoli et al., 2016). SEM provides the necessary magnification for visualisation of the fine-scale details of the EF network, but collagen fibres and ECM obscure the EF network in discs. A partial alkali digestion protocol, consisting of sonication in sodium hydroxide (NaOH) and heat treatment in 70°C water, removing ECM and collagen fibres allowed for clear visualisation of the EF

network under SEM (Tavakoli and Costi, 2018a, Tavakoli and Costi, 2017). No other study has visualised EF at this level of detail to obtain information on their ultrastructure.

In the partial alkali digestion technique that was developed by Dr. Javad Tavakoli, sheep AF samples were digested and then visualised under scanning electron microscopy. Briefly, NaOH and sonication was used to remove the ECM followed by a hot water (70°) bath to partially remove the collagen fibres. The EF network could be visualised in various regions of the AF with the highest density of EF found in the ILM region. Within the lamellae, the EF were parallel to the collagen fibres. Between the lamellae (i.e. within the ILM), a dense network existed consisting of two different sized fibres where thicker fibres were interconnected by finer fibres (Tavakoli and Costi, 2018a, Tavakoli and Costi, 2017). The EF structure and density using the partial digestion method was found to be similar to previously published results using light microscopy (Tavakoli and Costi, 2018a, Yu, 2002, Mikawa et al., 1986). However, the network structure of EF had never been described before in any previous study. Due to the high resolution of the images obtained from SEM, these images could be quantitatively analysed using an image analysis software called ImageJ.

Using ImageJ, the EF were converted to a binary (8-bit) image, where the EF were black and the background was white, allowing for analysis of EF distribution and angle (Tavakoli and Costi, 2018a). Comparing SEM images to images that were obtained from light microscopy, images obtained from the SEM allowed for better quantitative analysis in binary compared to the light microscopy images which were hard to distinguish between EF and background. Statistical analysis revealed significant differences in fibre angle in digested samples (where samples were sonicated and heat treated) compared to control samples (where samples were only sonicated) (Tavakoli and Costi, 2018a). These differences indicate that the heat treatment stage of the alkali digestion protocol affects the angle of the EF.

Microstructural changes in the disc, characteristic of disc degeneration, can result in delamination of the AF that can lead to mechanical property changes and herniation. It is therefore important to investigate the mechanisms that maintain the structural integrity of the disc. In the ILM, the major component is EF. EF have been found to create a dense network that merges into the lamellae with mechanical properties that match their ultrastructure. In order to increase understanding of the mechanisms by which herniation and lower back pain occur, the structure and function of EF must be investigated in human IVD.

Gaps Analysis

Structure and functional role of EF in human intervertebral discs is necessary for understanding pathways to herniation and disc degeneration. However, previous research on visualisation of the EF has either only been done using animal models or by light microscopy. A complete study of the structure and function of EF should include high resolution SEM imaging for visualisation and micromechanical testing on a digested AF sample containing isolated EF. Isolation of the EF network within a lamellae-ILM-lamellae sample to measure EF mechanical properties can only be conducted after the technique for isolating the EF network has been optimised for use in human AF samples. Although enzymatic treatments have shown success in determining the effect of removing the EF network from intervertebral discs, non-specific degradation of other components in the AF was difficult to limit (Smith et al., 2008). Enzymatic treatments are also expensive and time-consuming. Therefore, the partial alkali digestion protocol is preferred for determining the mechanical properties of EF in intervertebral discs.

Due to time constraints on the length of this project as well as the effect of COVID-19 on access to laboratories and equipment, only optimization of the partial alkali digestion protocol will be conducted to visualise EF ultrastructure in human AF. Future studies should aim to conduct micromechanical tests on a digested lamellae-ILM-lamellae sample for further insight into the functional role of EF. Mechanical properties of the EF network in the ILM, however, have been found to be consistent with the ultrastructure of EF visualised by SEM after partial alkali digestion (Tavakoli and Costi, 2018b, Tavakoli and Costi, 2018c). Therefore, the function of EF can be inferred within the scope of this project based on the ultrastructural organization of EF in human intervertebral discs.

Aim

Visualisation of EF using partial alkali digestion has only been investigated in sheep AF samples. However, the clinical relevance of the EF network can only be interpreted using human samples. Since the constituents of the disc is the same between species, but in varying concentrations, the partial digestion protocol can also be used to visualise the EF in human discs. EF have been visualised in human AF samples using this partial alkali digestion with an increase in duration of both sonication time and hot water treatment compared to the method used in sheep samples (Tavakoli and Costi, 2018a).

The first aim of this study was to verify the partial digestion protocol in sheep AF samples and the second aim was to optimise the partial digestion protocol for use in human AF samples to further investigate the structure and function of EF. The optimization protocol initially consisted of varying the duration of sonication because increasing sonication time has allowed for better visualisation of EF (Tavakoli and Costi, 2018a). It is important to note, however, that increasing the sonication time can also result in complete digestion of the sample preventing visualisation of EF. Due to the difference in the concentration of the components of human discs, the concentration of the NaOH was also changed to better visualise the EF network. Optimization of the digestion protocol will allow for investigating the variation in the density and organization of EF based on the region in the disc, the level of the disc, and degeneration grade. Developing a detailed understanding of the structure and function of EF in human discs will provide new insights into mechanisms of disc degeneration, herniation, and back pain.

Materials and Methods

Aim 1- Sheep EF Visualisation

For the first aim, sheep lumbar spine was thawed and tissues surrounding the intervertebral discs were removed with a surgical blade. Using a feather blade, one L5/L6 intervertebral disc (Merino Wether approximately 12 months old) was isolated from the surrounding vertebral bodies. After spraying the disc with saline solution, it was stored at -20°C to freeze. Once the disc was frozen again, an anterior section (1cm x 1cm) was cut using a surgical blade. An anterior section was used as per the methodology described by Dr. Javad Tavakoli. Using optimal cutting temperature compounds (OCT), the disc section was mounted on the cryostat microtome specimen holder at 60° from the vertical axis. This angle was chosen because it is the approximate angle of the collagen fibres in the lamellae which assists in identifying the lamellar and ILM region under the SEM. Samples were cut from the disc at 30µm using the cryostat microtome and stored in a petri dish at -20°C until the partial digestion.

All samples were placed in 700mL 0.5M NaOH in a Pyrex beaker and the beaker with the samples was placed in the ultrasonic processor. This volume of NaOH was used in order to mimic sink conditions so that the debris that is removed from the samples during sonication does not change the concentration of the NaOH. Sonication was performed on the samples for 25 minutes at 25kHz with on and off times of 2s and 0.5 seconds respectively with the amplitude transformer set to ϕ3 at room temperature to remove ECM.

After sonication, the samples were removed from the sonication beaker and placed in 500mL of distilled water for 5 minutes to further encourage hydrolysis of fibres and other proteins in the ECM. Once the samples had been soaked in distilled water, they were placed in 200mL of 70°C distilled water for 5 minutes to remove collagen. Samples were then partially dehydrated using increasing concentrations of ethanol. Specifically, samples were added to 100mL of 30% ethanol in a petri dish for 2 minutes. Then the 30% ethanol was replaced with 70% ethanol using a syringe, carefully making sure to not spray ethanol directly onto the samples, and left for 2 minutes. Finally, the 70% ethanol was replaced with 90% ethanol for 30 seconds.

Double adhesive carbon tape was used to secure the samples on aluminium (Al) stubs. The Al stubs were kept on a microtube rack to ensure that they stayed upright and the microtube rack containing the Al stubs were placed in a vacuum oven at -80kPa and 37°C overnight for

at least 5 hours. After the samples had dried, they were sputter coated with 2nm platinum at 25mA and visualised by SEM.

Initially, samples were scanned at a lower magnification to find areas of digestion. Since intervertebral discs are not homogenous, the partial digestion will not occur the same in all of the areas on all of the samples. Once a digested region was located based on the formation of fenestrations or holes, magnification was increased to locate EF. Voltage was not increased above 10kV in order to prevent damaging the samples or breaking the EF network and spot size was varied between 2 and 5 to find a balance between removing noise while maintaining high resolution.

One variation experiment was conducted using sheep AF, (that showed success in removing collagen and ECM), prior to trialling the alternate method in the optimization of the digestion protocol on human samples (Ushiki, 2002). In this variation, instead of using a hot water post sonication treatment, 70°C 0.5M NaOH was used as a pre-sonication treatment to remove collagen fibres and encourage digestion. Samples were soaked in the hot NaOH for 2 minutes, 4 minutes, 6 minutes, and 10 minutes prior to sonicating in room temperature NaOH for 25 minutes as the original protocol indicated.

Aim 2- Human EF Visualisation

To optimize the visualisation of EF in human discs (second aim), a series of experiments were conducted varying one parameter to better reveal the EF network as demonstrated in sheep samples (Table 1). Based on the results of previous experiments conducted on sheep, indicating that longer sonication time lead to increased digestion, the initial experiment varied sonication duration using human AF samples. Each experiment aimed to optimize the digestion protocol such that the EF network was not obscured by other AF constituents or damaged during the procedure. Variations from the original protocol are summarized in Table 1. Prior to sample preparation, the discs of interest had to be located in the cadaver freezer at Tonsley and graded for degeneration using magnetic resonance imaging (MRI) scans and the Pfirrmann Grading System (Pfirrmann et al., 2001). Based on the available discs and their degeneration level, the L1/L2 disc level was chosen. Discs with a low degeneration grading were preferred, meaning the discs chosen were mostly healthy, since degenerated discs have previously shown disruption to the EF network. Two discs (31 year old male and 53 year old male) were isolated using the same methodology described in the Sheep EF Visualisation. Then anterior or lateral sections were sectioned by cryostat microtome prior to each experiment. Regions of interest was chosen based on whether a 1cm x 1cm section could be cut from the sample with the lamellar sheets mostly parallel. Thickness of the sample was maintained at 30µm for all experiments, but samples were cut horizontally as well as obliquely (60° from the vertical axis) for two experiments. Otherwise, all samples were only cut obliquely. Ultrasonic processor settings also remained the same as for the sheep protocol. In each of the human sample experiments, the hot water post treatment was done for 12 minutes as specified by Dr. Javad Tavakoli for human AF samples. Partial dehydration process and vacuum oven drying remained the same for all of the human sample experiments as for the sheep samples. SEM imaging technique also remained the same as for the sheep AF samples across all of the experiments.

In the first experiment for optimization of digestion protocol, the effect of sonication time was tested. Lateral disc AF samples were placed in 700mL 0.5M NaOH and sonicated for 15 minutes (N=1), 20 minutes (N=1), 45 minutes (N=1), and 60 minutes (N=1). Then in the second experiment, lateral disc section samples were cut obliquely (N=2) and horizontally (N=2) then sonicated in 700mL of 1.0M NaOH for 30 minutes. In the third experiment, lateral disc section

samples were cut horizontally and obliquely then soaked in 1.0M NaOH overnight (>12 hours) in two separate beakers (one for each cutting angle) at room temperature. The following day, the beaker with the horizontally cut samples were sonicated for 30 minutes (N=2) and 60 minutes (N=2). Then the beaker containing the obliquely cut samples were sonicated for 30 minutes (N=2) and 60 minutes (N=2). In the final experiment, anterior disc sections were sonicated for 60 minutes (N=2), 90 minutes (N=2), and 120 minutes (N=2). Note that the sample numbers are the quantity of samples that were visualised under SEM. Many more samples were prepared and sonicated to ensure samples would be available for visualisation by SEM (some samples disappeared in the solution or were damaged by sample mishandling).

Table 1. Experiments conducted on Sheep and Human AF Samples

Species	Experiment No.	Sample Preparation	Pre-Sonication	Sonication	Hot water treatment
Sheep	1	Anterior L5/L6 cut obliquely	None	0.5M NaOH for 25 minutes	5 minutes
Sheep	2	Anterior L5/L6 cut obliquely	70°C 0.5M NaOH for various times	0.5M NaOH for 25 minutes	None
Human	1	Lateral L1/L1 cut obliquely	None	0.5M NaOH for various times	12 minutes
Human	2	Lateral L1/L2 cut obliquely and horizontally	None	1.0M NaOH for 30 minutes	12 minutes
Human	3	Lateral L1/L2 cut obliquely and horizontally	Soaked in 1.0M NaOH overnight	1.0M NaOH for 30 minutes and 60 minutes	12 minutes
Human	4	Anterior L1/L2 cut obliquely	None	1.0M for 60 minutes, 90 minutes, and 120 minutes	12 minutes

Results

Aim 1- Sheep EF Visualisation

Sheep Sample Experiment 1

Sheep EF visualisation partial digestion protocol, summarized in Table 1, was conducted as described by Dr. Javad Tavakoli. Two trials were conducted to replicate this protocol. In the first attempt, the hot water post treatment had not reached 70°C because the beaker with the water was placed in a water bath. Therefore, a second attempt was undertaken where the beaker with water was placed in an oven set to 80°C prior to sonication, to ensure that the temperature of the water was hot enough to remove the collagen fibres.

Visualisation of EF in the first attempt was difficult and no images of EF were obtained from the SEM. Sheep AF samples had reduced in size and changed in shape when they were transferred to the Al subs, compared to their prepared size of 1cm x 1cm, and no distinguishable features such as the lamellae could be seen (Figure 4).

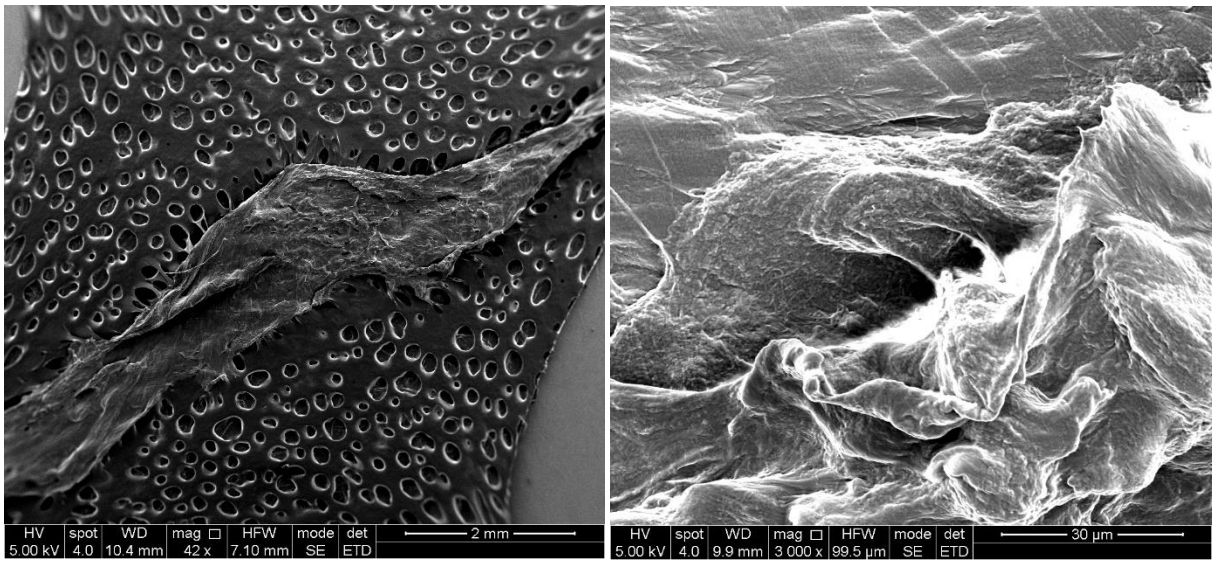

Figure 4. SEM images from the first attempt at Sheep Sample Experiment 1. Both images are from the same sample. Left: zoomed out picture of sample on the Al stub. Background with holes is the carbon tape, sample can be seen in the center of the tape. Right: zoomed in picture showing folds in the sample and lack of distinguishable features.

Other digested samples had tears. Fibrous components were visible in the sample, but none of these were EF (Figure 5). No sequential images (from zoomed out to zoomed in) were obtained for any of the fibrous components. Lack of images of the surrounding area and the lack of distinguishable features made it difficult to determine if the images were obtained from the lamellae or ILM region.

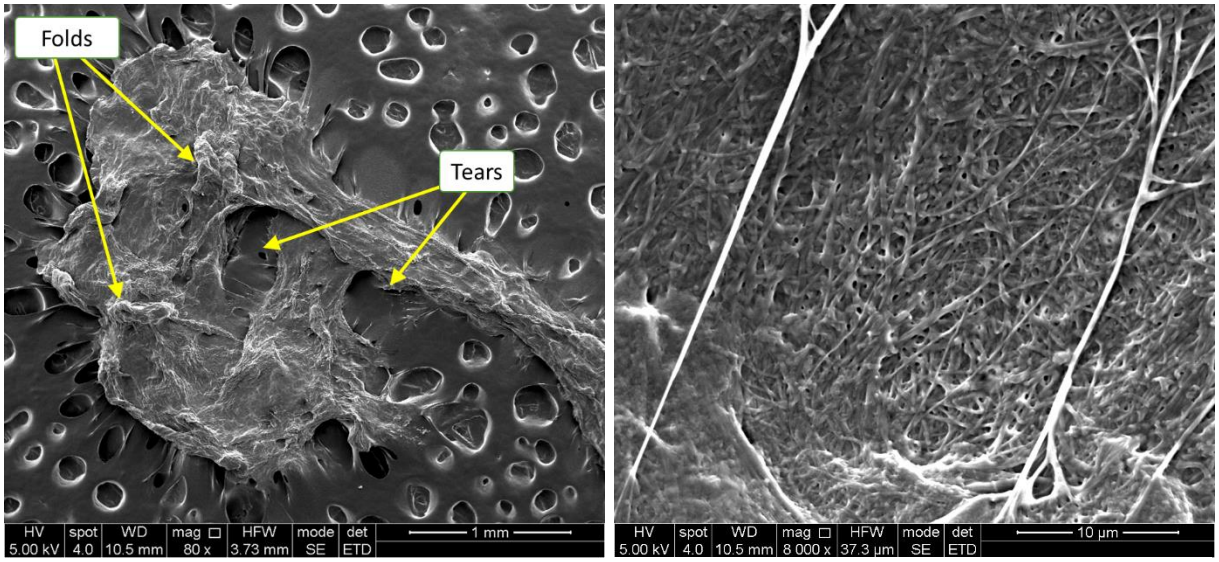

Figure 5. SEM images from the first attempt at Sheep Sample Experiment 1. Both images are from the same sample. Left: holes and tears can be seen in the image. Right: fibrous components.

In the second attempt, extra care was taken to ensure that the samples were handled such that they were flat on the Al stubs, and to limit sample damage (i.e. tears). Using forceps to pick up the sample from the ethanol, in the final partial dehydration stage, led to the sample becoming curled around the tip of the forceps. When the sample was then transferred from the forceps to the Al stub, the sample remained curled leading to folds in the sample. Therefore, a small metal spoon was used to transfer the samples onto the stubs rather than forceps.

Samples were successfully placed flat on the Al stubs, in the second attempt, such that each lamellar sheet could be determined from the samples under the SEM (Figure 6). Since the samples were cut at 60° from the vertical axis (the approximate angle of the collagen fibres in the lamellae), lamellae observed as untextured, flat areas were in-plane lamellae (describing the angle of the collagen fibres). Areas that were not flat were regions where the collagen fibres were cut at an angle and make the cross-sectional collagen bundles in the lamellae visible as ridges. Digested areas were observed as regions where small fenestrations or holes were visible in the sample. These areas were where EF would be located as the collagen fibres and ECM were removed creating these spaces where only EF would remain.

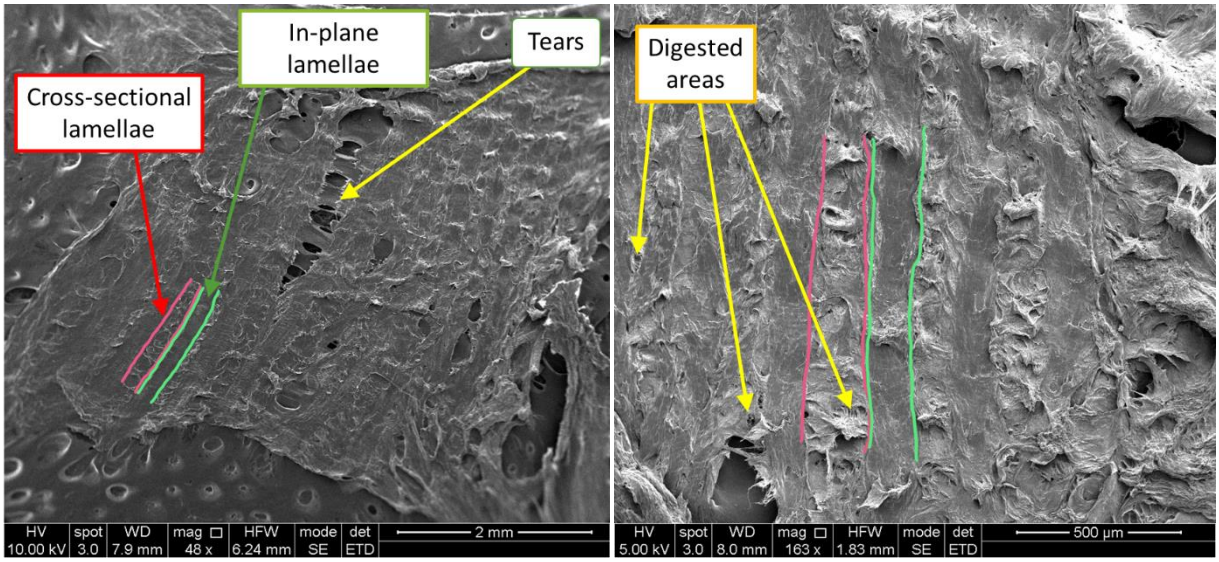

Figure 6. SEM images from second attempt at Sheep Sample Experiment 1. Images are of two different samples. Areas within the green lines show in-plane lamellae and areas within the red lines are cross-sectional lamellae. Digested areas are indicated by yellow arrows in the image on the right.

Sheep sample experiment 1 was the first time that SEM imaging had been attempted. In the second trial of this experiment, EF were visualised. Fibres were determined to be EF based on relative size to surrounding fibres and from the lack of other fibrous components in digested areas. Two different sizes of EF were visualised, one larger and one finer (Figure 7). Thinner EF appeared to connect larger fibres since the thinner EF spanned between two thicker fibres. No sequential images were taken therefore there was no definitive information on the surrounding area. Therefore, location of the EF can only be inferred from their orientation.

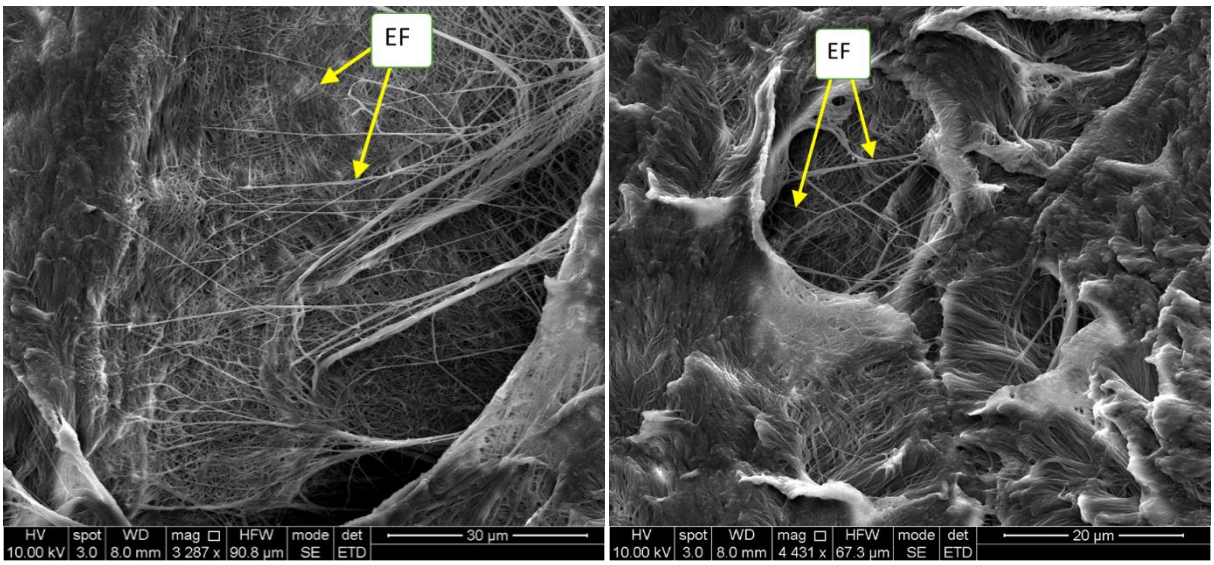

Figure 7. SEM images from second attempt at Sheep Sample Experiment 1. Images are from two different samples. Both images show EF. Two different sizes of EF can be seen.

Sheep Sample Experiment 2

In sheep sample experiment 2, the samples were treated with hot NaOH prior to sonication (Table 1). During sonication, samples had separated into smaller pieces that could be seen floating in the beaker. In the right image in Figure 8, the change in size of the sample is evident. Similar to Figure 5, the background with the holes was the carbon tape. Samples were prepared to be 1cm x 1cm, but after sonication the sample that was obtained was not the same size. The sample that was pre-treated in NaOH for 2 minutes was extensively examined for presence of EF, but none were found. Due to time constraints (as the SEM had only been reserved for two hours), the sample that was analysed next was the one that had been pre-treated in NaOH for 10 minutes to obtain information on the most significant effect of the hot NaOH.

The smaller size of the sample that had been hot alkali treated for 10 minutes meant that there were not many locations to look for EF. No distinguishable structural components or digested areas were visible in the sample that had been pre-treated for 10 minutes (Figure 8). Surface of the sample that had been hot alkali digested was different from the samples that followed the original protocol as seen in Figure 6. Bubbles were observed in the sample that

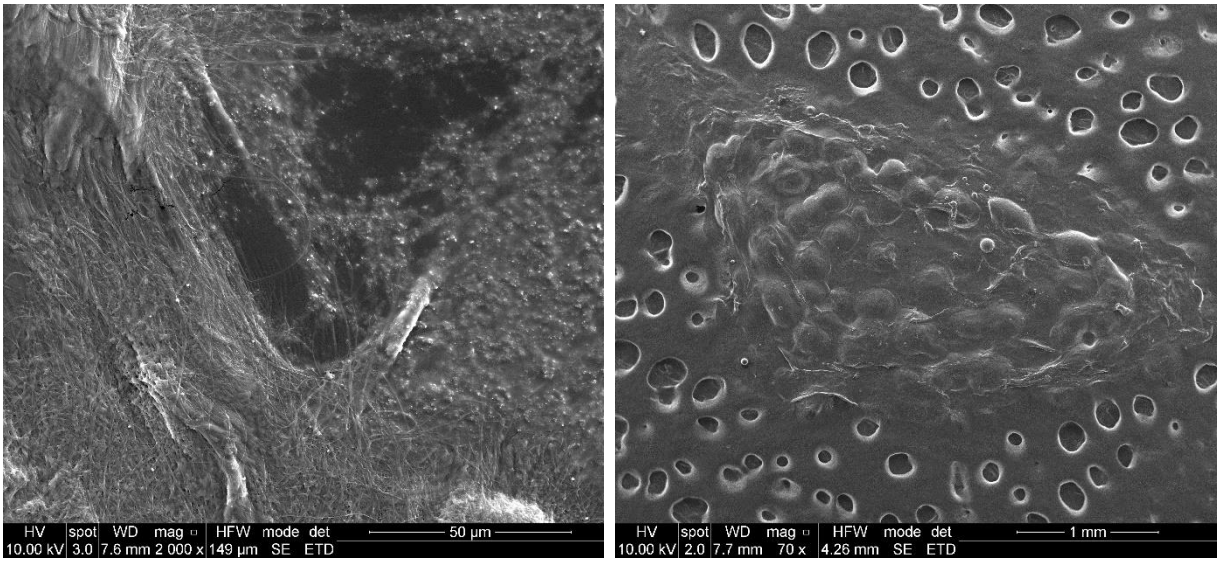

Figure 8. SEM images from Sheep Sample Experiment 2. Images are of two different durations of hot alkali digestion. Left: Sample pre-treated for 2 minutes. Right: Sample pre-treated for 10 minutes. Samples were much smaller than initially prepared, verified by the scale bar, and did not have any visible structural components.

had been sonicated for 10 minutes after the hot alkali treatment. No sample that had been previously imaged under the SEM had these bubbles. All other samples that had been pre-treated for the other durations were not visualised by SEM due to time constraints.

Since EF were visualised in the second attempt of sheep sample experiment 1, the optimization stage could commence using human samples. Using the original protocol as described by Dr. Javad Tavakoli, EF were visualised under SEM in sheep samples, as can be seen in Figure 7. Sheep experiment 1 was important to ensure that the original protocol could be replicated to reduce the effect of human error on the optimization process prior to changing variables in the protocol for use in human AF samples. Further images of all experiments conducted in the sheep trials can be found in Appendix A.

Aim 2- Human EF Visualisation

The main aim of this project was to optimise the partial alkali digestion protocol for use in human AF samples. A series of experiments were conducted that tested the effect of sonication time, pre-treatment, and concentration of the NaOH solution on the visibility of EF in human intervertebral discs (Table 1). Previously published results showed that increasing sonication time had a positive relationship with EF visibility (until the optimal time was reached and then the sample becomes over-digested). Therefore, the first experiment tested different durations of sonication.

Human Sample Experiment 1

Human AF samples that were digested for 15 minutes, 45 minutes, and 60 minutes can be seen in Figure 9. Lamellar sheets were not as easily observed at a low magnification compared to the sheep samples that were digested similarly. However, in images of a higher magnification, the cross-sectional and in-plane lamellae could be seen (Figure 11). In the sample that was digested for 45 minutes, bubbles could be seen under the sample similar to the sheep AF samples that were hot alkali pre-treated. None of the samples from the first human experiment changed in size or separated into smaller pieces during sonication. Digested regions were not observed clearly from a low magnification and therefore the sample had to be scanned for these regions at a higher magnification.

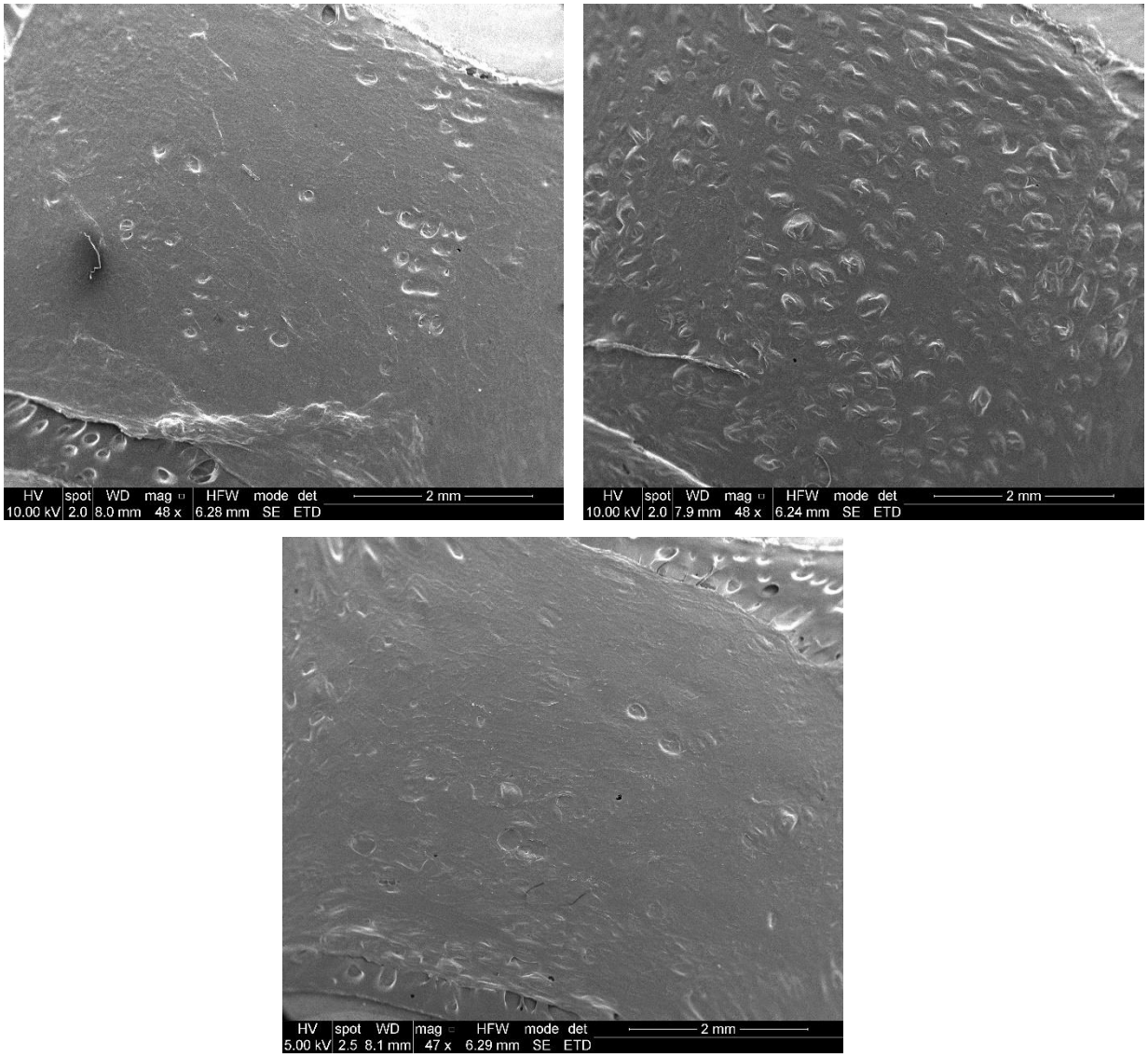

Figure 9. SEM images from human sample experiment 1. All images are from different samples. Top left: sample sonicated for 15 minutes. Top right: sample sonicated for 45 minutes. Bottom: sample sonicated for 60 minutes. Lamellar sheets cannot be easily distinguished at a low magnification.

Longer sonication time did not always increase digestion (Figure 10). The sample that was sonicated for 30 minutes had less visible fibrous components compared to the sample that was sonicated for 15 minutes. In the sample that was sonicated for 15 minutes, fibrous components and disruption to the surface of the sample can be seen (as a result of digestion) compared to the sample that was sonicated for 30 minutes. EF were only found in the sample that was sonicated for 60 minutes.

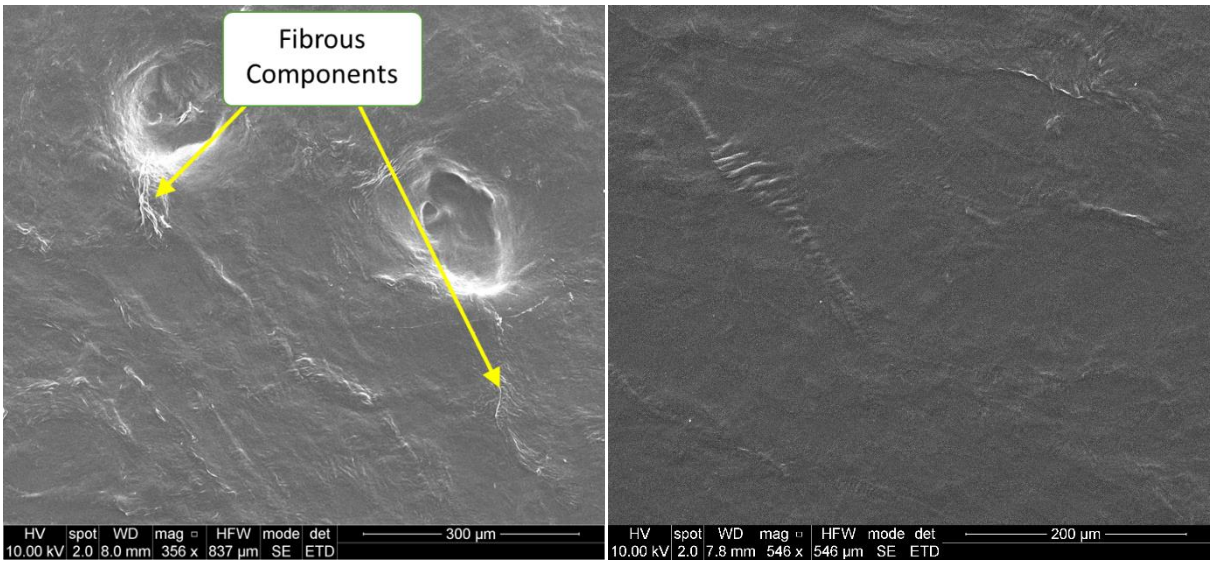

Figure 10. SEM images from human sample experiment 1 zoomed in. Both images are from different samples. Left: sample that was sonicated for 15 minutes. Fibrous components can be seen. Right: sample that was sonicated for 30 minutes.

In the sample that was digested for 60 minutes, EF were visualised towards the edge of the sample (Figure 11). Sequential images (from zoomed out to zoomed in) were taken of the EF providing information on the area surrounding the EF. Based on the in-plane lamellae and cross-sectional lamellae, the EF observed in Figure 11 were at the boundary between the ILM and the cross-sectional lamellae. Some of the EF in this region were exposed, however, EF closer to the ILM region were covered by ECM. EF can be seen through the ECM. The EF that were partially exposed in the ILM region did not run in the same direction as the EF found closer to the lamellar region. However, the EF that were in the cross-sectional area were mostly oriented in the same direction as each other, considering that the heat treatment process had a significant effect on the EF angle. After sonication for 60 minutes, the partial digestion protocol had exposed EF towards the edge of the sample.

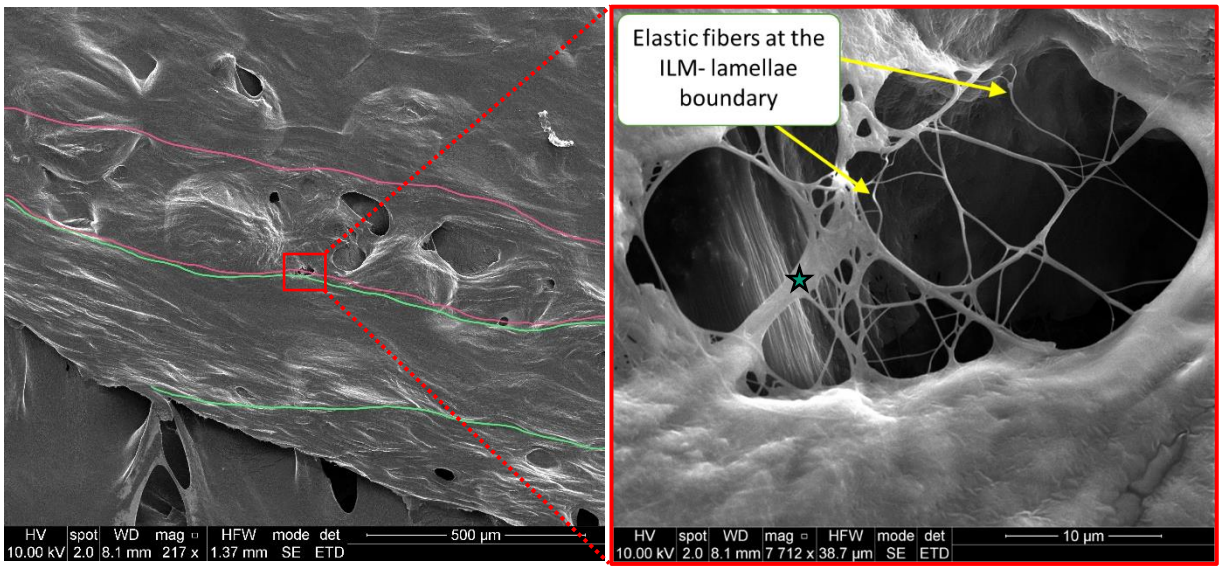

Figure 11. Sequential SEM images from human sample experiment 1. Both images are from the sample that was digested for 60 minutes. Left: zoomed out image of the EF location. Area within pink lines are cross-sectional lamellae and area within green lines are in-plane lamellae. Right: zoomed in picture of the EF. Star indicates undigested ECM.

Human Sample Experiment 2

Experiment 2 for the human samples tested the effect of increasing the concentration of the NaOH to 1.0M. Two different cutting angles were also used (horizontal and oblique) to explore any possible effect of cutting angle on the effectiveness of the digestion protocol. SEM imaging was done twice on two separate days because no EF were found on the first day. On the second day of SEM imaging, EF were found at the edge of the sample (Figure 12). Samples that were cut horizontally did not have in-plane lamellae because all the lamellae were cross-sectional. However, a difference was observed in the surface where the direction of the collagen bundles changes between the lamellar sheets. Since EF were only found at the edge of the sample, it is unclear whether this area was ILM or lamellar.

EF found in the horizontally cut sample that was sonicated using 1.0M NaOH were primarily in one direction, but other EF can be seen that connect these longer strands. Stars indicate undigested matrix in that cover the EF (Figure 12). Information about the size of the EF could not be clearly obtained due to the presence of the matrix obscuring the EF. However, EF strands were observed interconnected by other strands creating a mesh network organization.

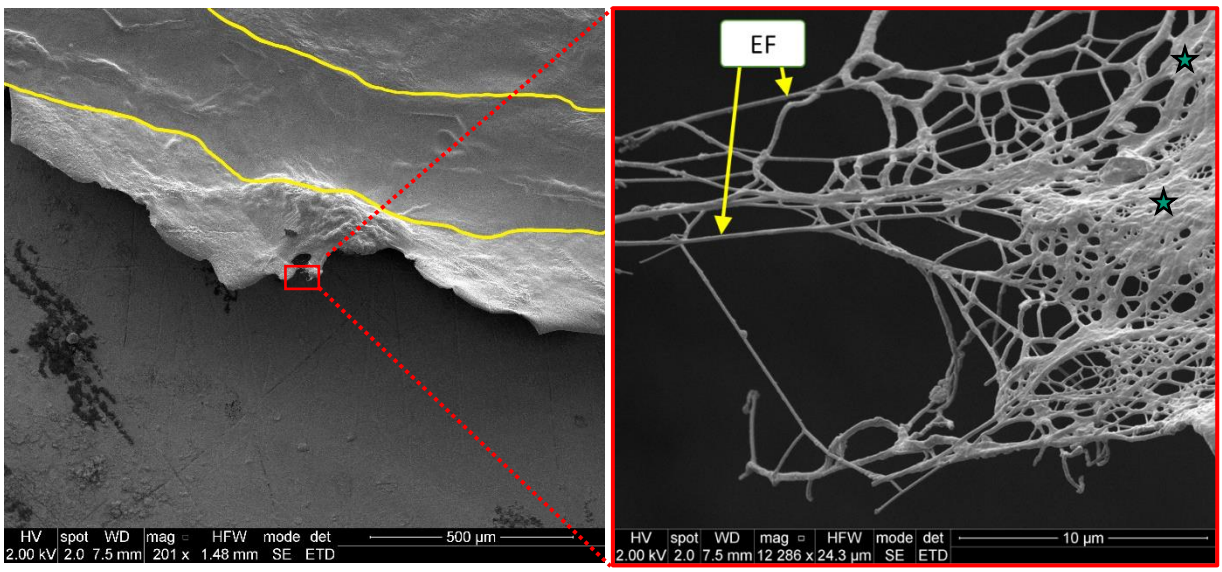

Figure 12. Sequential SEM images of human sample trial 2. Both images are of the same horizontally cut sample. Left: zoomed out image of the EF location. Lamellae boundaries are indicated by yellow lines. Right: zoomed in image of the EF. Star indicates undigested matrix.

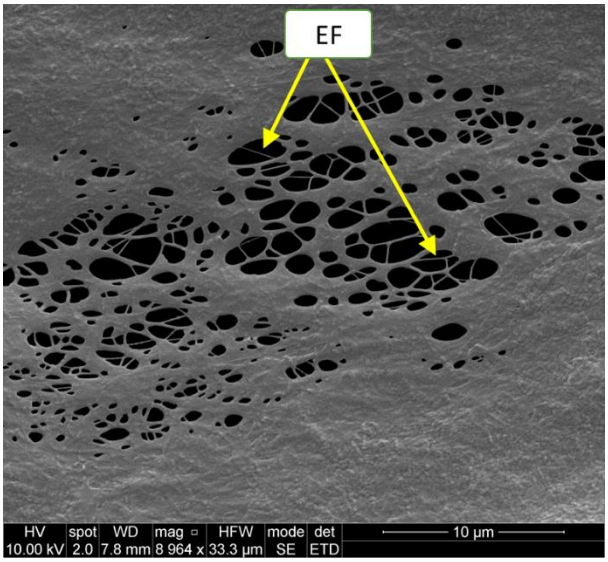

Figure 13. SEM images from human sample experiment 2. EF can be seen through holes where digestion has started.

EF obscured by undigested matrix were observed in an obliquely cut sample as well (Figure 13). Digestion had occurred for long enough to expose EF through small openings, but not enough to obtain information about the structure of the EF. Increasing the concentration of the NaOH to 1.0M did not heavily damage the samples, compared to the hot alkali treatment that resulted in samples that were torn during digestion. EF were observed in both oblique and horizontal samples. In order to digest more ECM, the samples were soaked in 1.0M NaOH overnight to encourage loosening of the matrix from the EF prior to sonication.

Human Sample Experiment 3

Prior to sonication, the samples that had soaked in NaOH overnight were translucent at the edges. After sonicating for 15 minutes, samples had separated and bits of samples were seen floating in the sonication beaker. However, since the previous sonication had undigested ECM obscuring the EF network, the sonication occurred to completion at 30 minutes or 60 minutes. In both the horizontal and obliquely cut samples, the number of samples that were comparable to the original size at which they were prepared had decreased.

EF were not found in the oblique or horizontally cut samples. No images were obtained of the samples that had been sonicated for 60 minutes. Tears and an untextured surface similar to undigested samples were observed in the samples with no distinguishable structural components (Figure 14). SEM imaging was only done on one day and the samples were not rescanned

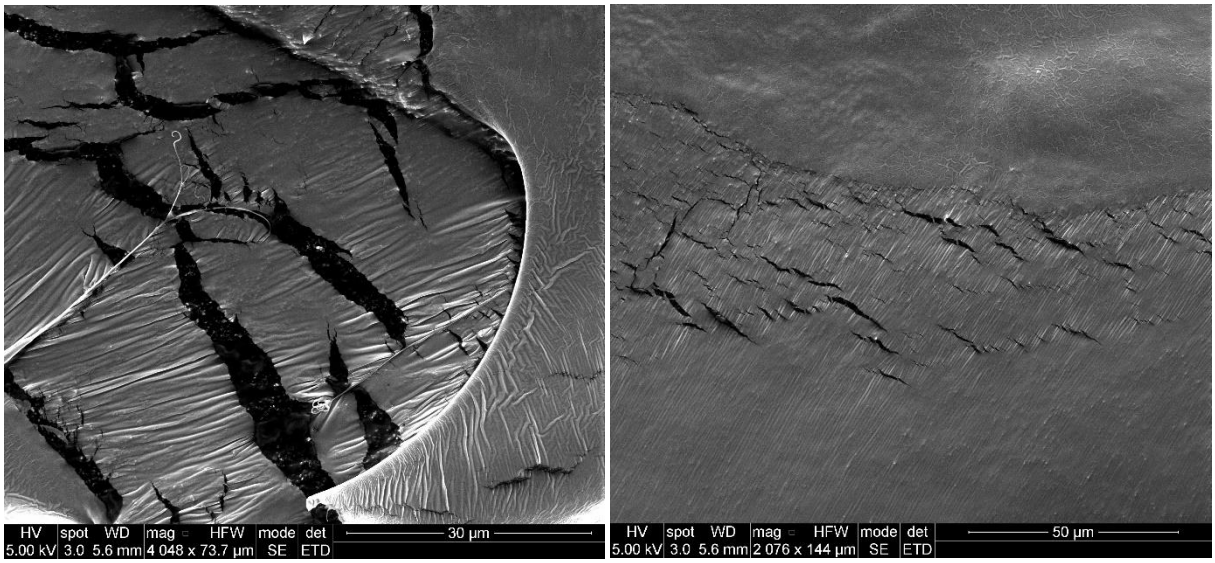

Figure 14. SEM images of human sample experiment 3. Both images are of obliquely cut samples that were soaked in 1.0M NaOH and sonicated for 30 minutes. Left: tears can be seen in the samples. Right: samples were untextured and looked similar to undigested samples.

Human Sample Experiment 4

A slower process of digestion was explored in the next step where samples were sonicated in 1.0M NaOH for 60 minutes, 90 minutes, and 120 minutes. Samples were imaged on two

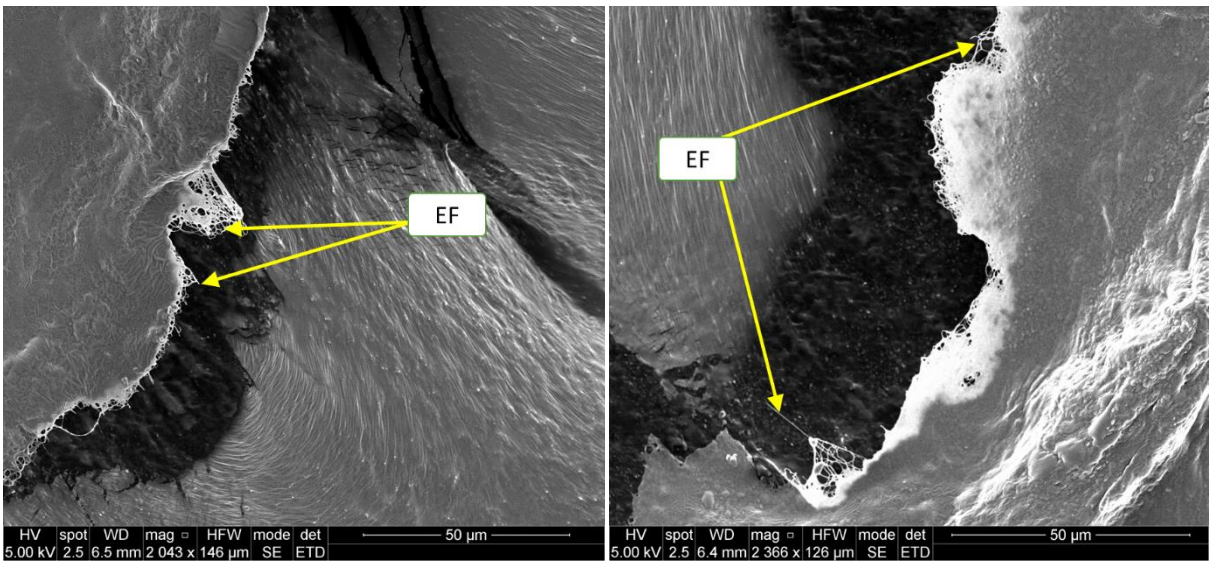

Figure 15. Incomplete or torn EF from human sample experiment 4 sonicated for 60 minutes and 90 minutes. Images are from two different samples. Left: sample that was sonicated for 60 minutes. Right: sample that was digested for 90 minutes.

different days by SEM. Incomplete or broken EF were observed in samples that were digested for 60 minutes and 90 minutes. During SEM imaging, single EF could be seen recoiling live (no images). Due to the EF in these locations being incomplete or torn, no sequential images were taken of surrounding areas at a lower magnification. In the samples that were sonicated for 120 minutes, complete EF could be seen more clearly.

Samples that were sonicated for 120 minutes were visualised under SEM on two different days because EF were found on the first day and the whole sample had not been scanned extensively. On the second day, only the samples that were sonicated for 120 minutes were visualised as it showed the most successful digestion compared to the other samples that had been digested for 60 and 90 minutes.

In the samples that were sonicated for 120 minutes, the lamellar sheets can be observed at a higher magnification (Figure 17). EF were observed in the lamellar sheet towards the ILM side primarily oriented in the same direction. Undigested matrix obscured the EF network on the side away from the ILM making it difficult to definitely obtain information on the size of the EF that were seen in this location.

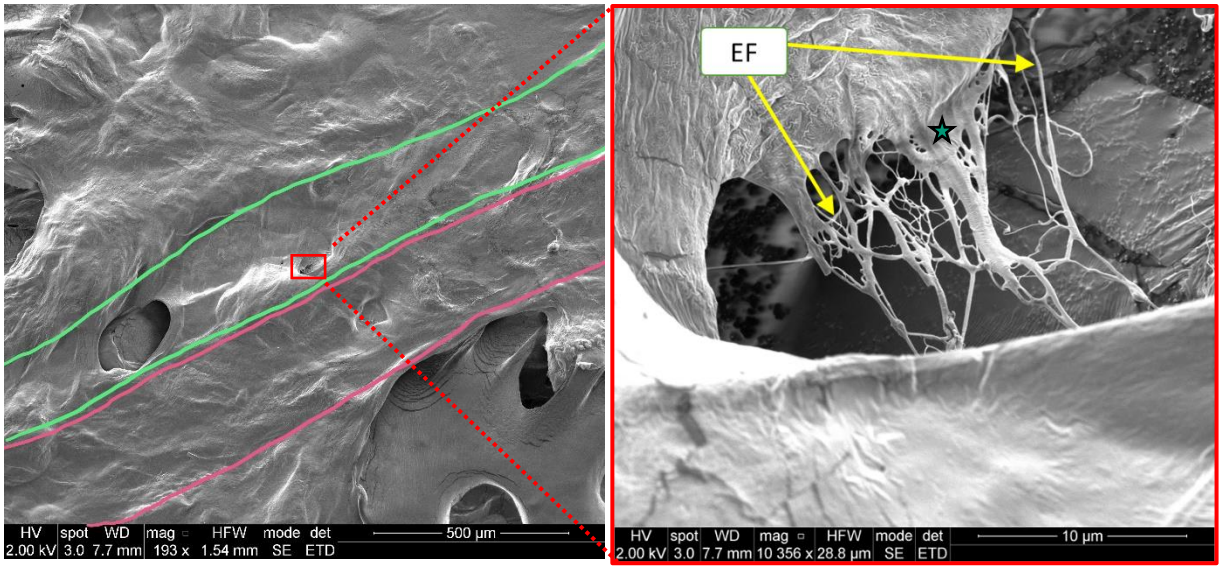

Figure 17. SEM images from human sample experiment 4 sonicated for 120 minutes. Both images are from the same sample. Left: zoomed out image showing in-plane (green) and cross-sectional lamellae (pink). Right: zoomed in picture of location outlined in the left images showing EF. Star shows undigested matrix.

EF were also found at the edge of the sample that was sonicated for 120 minutes. Due to the location of the EF being at the very edge of the sample, information about the surrounding area could only be obtained from one side. Therefore, location of the EF is hard to determine as being in the lamellae or the ILM region. However, EF of two sizes can be clearly distinguished (Figure 16).

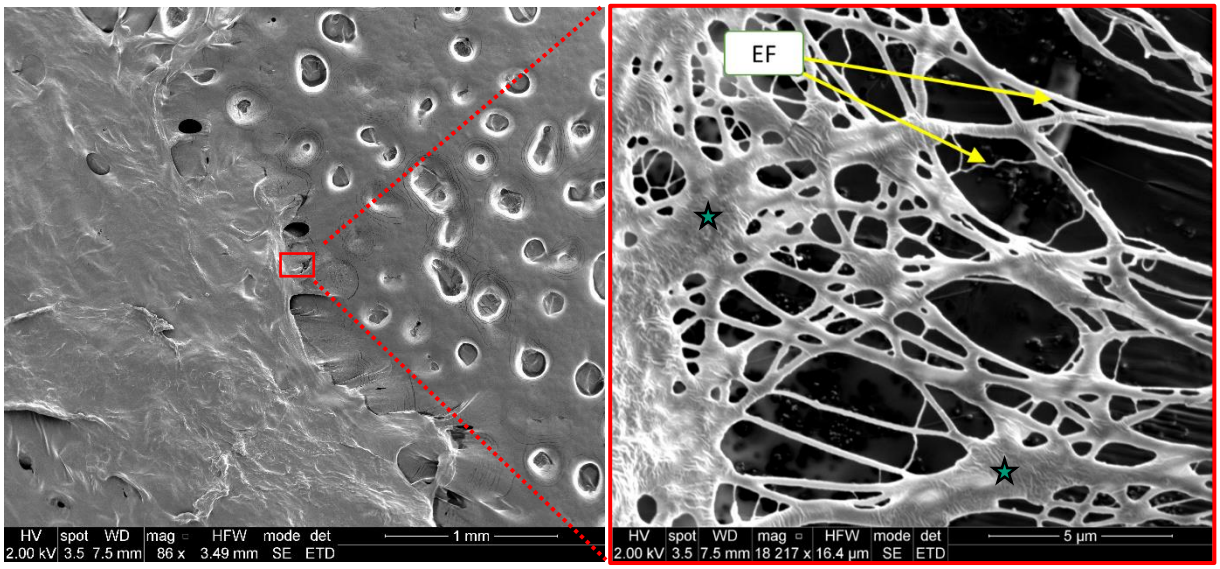

Figure 16. SEM images from human sample experiment 4 sonicated for 120 minutes. Both images are from the same sample. Left: zoomed out image showing location of EF. Right: zoomed in picture of the area outlined in the left image.

In Figure 16, larger EF fibres can be seen that were mostly oriented in the same direction connected together by finer EF. Undigested matrix on the left side of the image obscured the

structure of the EF. However, the sample had been digested enough to reveal the EF that create a network structure that had larger fibres that were connected together by finer fibres.

Structure of the EF and the location at which that were found in the human AF samples can be used to infer the function of EF. Location of the EF was only determined definitively if sequential images had been taken that showed the region that surrounded the EF. In some cases, since the EF were located at the edge of the sample, the location at which the EF were located could not be determined since structural components of the disc can only be seen in one side of the sample. EF were observed in the lamellae primarily of one size that were all mostly parallel to each other. In other regions where EF were located in human samples, larger fibres can be seen that were interconnected by finer fibres which is similar to the structure of EF that was found in the sheep AF samples. Undigested matrix can be seen obscuring the EF in the samples, however, locations where ECM was removed can be located. Locating regions where EF were exposed where collagen and ECM have been removed to expose only the EF was done across two different days of SEM in some experiments. In other experiments, conducting SEM imaging again did not seem worthwhile from the images that were obtained on the first day. Replicating the original study that was done on sheep AF samples decreased the effect of learning the technique and human error during the optimization stage.

Discussion

The structure and function of EF in human intervertebral discs can provide new insights into the mechanisms of disc degeneration and herniation. This project aimed to optimise a partial alkali digestion protocol for use in human AF samples that was initially developed for visualisation of EF in sheep AF samples. A two-step process was undertaken to optimise this procedure. First, the original protocol that was developed for sheep AF samples was replicated. In the next stage, various parameters of the partial alkali digestion protocol were changed (sonication time, concentration of NaOH, and pre-treatment) to visualise the ultrastructure of EF in human AF samples.

In the first stage of this project, execution of the methodology was the limiting factor in the success of visualizing EF. Sheep experiment 1, Table 1, shows the difference that the correct implementation of the protocol can make in visualisation. Although the experiment followed the instructions specified in the first trial, alternate techniques than what had been used in the original study yielded more successful results in the second trial (Figure 4, Figure 6). In the study that described the digestion protocol for sheep samples, forceps were used to transfer of the sample onto the Al stubs. However, using forceps caused the sample to curl around the tip of the tool, which led to folds in the sample or sample tears when attempting to flatten it on the Al stub (Figure 5). Tears were observed in the sample that was transferred using a small spoon in the second trial, but larger areas around the tear existed that were not damaged (Figure 6). Sample tears could damage the EF network and/or the surrounding structures that the EF use to anchor. Both of these consequences of sample tears can lead to unsuccessful visualisation of the EF network.

Attempting to visualise the EF network in a sample that was not flat on the Al stub was not successful. Using a small spoon instead of forceps for sample transfer assisted in ensuring that the sample lay flat on the Al stub allowing better visualisation of the lamellar sheets on the sample and the EF network. In samples that were folded, the digested areas where EF were visible become difficult to locate for two main reasons. Firstly, there was no indication of the structures in the sample making it difficult to determine the ILM regions where EF are primarily located. Secondly, the digested areas could have existed within the folded regions that were not possible to view. In the second attempt of sheep sample experiment 1, the effect of the sample laying flat on the Al stub surface was evident since the lamellar sheets

could be easily distinguished from each other at a low magnification (Figure 6). Since the sample was sliced by cryostat microtome at the approximate angle of the collagen fibres and the angle of the collagen fibres alternates direction, flat areas were lamellar sheets with collagen fibres in-plane to the cutting angle and ridged areas were lamellar sheets where the collagen fibres were cross-sectional to the surface of the sample (Figure 5, Figure 11, Figure 17). EF that were located in the second trial could then be determined to be in the lamellae or the ILM region.

Fibrous components could be seen in the first trial of sheep experiment 1, but these fibres were likely collagen fibres rather than EF due to their structure and an error in post-sonication treatment procedure (Figure 5). In the first attempt, the hot water post-sonication did not reach the correct temperature leaving the collagen fibres intact. Collagen is not as heat resistant as EF and therefore it is vital that the post-sonication hot water bath reaches the correct temperature to remove the collagen fibres that obscure the EF network. The collagen fibres were clearly visible in the sample (Figure 5) because the sonication process occurred as expected and removed the ECM leaving behind unobscured collagen fibres. Visualisation of EF was increased in the second attempt due to the higher temperature of the hot water during the post-sonication step and better sample handling.

The purpose of the first stage of this project was to ensure the repeatability of the partial alkali digestion protocol using sheep AF samples. In the second attempt of sheep sample experiment 1, EF were visualised (Figure 7). It is likely that the EF that were found in this location were within the lamellae due to their orientation. Previously published data have described elastic fibres as being mostly parallel to each other and the collagen fibres in the lamellae (Yu et al., 2002, Tavakoli and Costi, 2018a, Tavakoli and Costi, 2017). Within the ILM, EF have been described to be interconnected by smaller fibres which were observed in the results that were obtained in this experiment. However, it is unclear whether the appearance of interconnecting fibres was due to a change in the orientation of the EF as a result of the post-sonication heat treatment. Further imaging would have resulted in increased visualisation of the EF network as many digested areas could be seen in the sample at a low magnification, but identification of areas to look for EF was a skill that was learned throughout the project.

Successful replication of the partial alkali digestion in sheep AF samples was accomplished in the second attempt of sheep experiment 1 (Table 1) after learning how to execute the protocol correctly and effectively. In the next stage of this project, this protocol was implemented with changes to individual variables to optimise visualisation of the EF network in human AF samples. Since previous research on EF in human intervertebral discs is limited, the results obtained from the experiments conducted during optimization cannot be easily validated. Therefore, it is important to ensure that the results obtained from an experiment were an effect of the changes implemented rather than incorrect execution of the protocol. By successfully replicating the partial alkali digestion protocol in sheep AF, the basic techniques (sample handling, correct use of equipment) were learned prior to the optimization stage. In the original study, the effect of increasing the sonication time on the visualisation of EF in sheep AF samples was investigated, but other experiments, such as increasing concentration of the NaOH, that were conducted in the optimization stage were not.

In the study that developed the partial alkali digestion technique, increasing sonication time was shown to improve visualisation of EF in sheep samples. Secondly, a longer sonication duration was mentioned for using this technique in human AF samples (Tavakoli and Costi, 2017). Therefore, the first experiment conducted in the optimization stage attempted to visualise EF in human AF by increasing sonication time. A longer sonication time (and a longer post-sonication heat treatment time) were required for visualisation of EF in human AF compared to sheep AF. Comparing the surface of the human AF samples visualised under the SEM at a low magnification to the surface of the sheep AF samples, the lamellar sheets cannot be easily distinguished (Figure 18). However, at a higher magnification, the lamellae can be approximated (Figure 11).

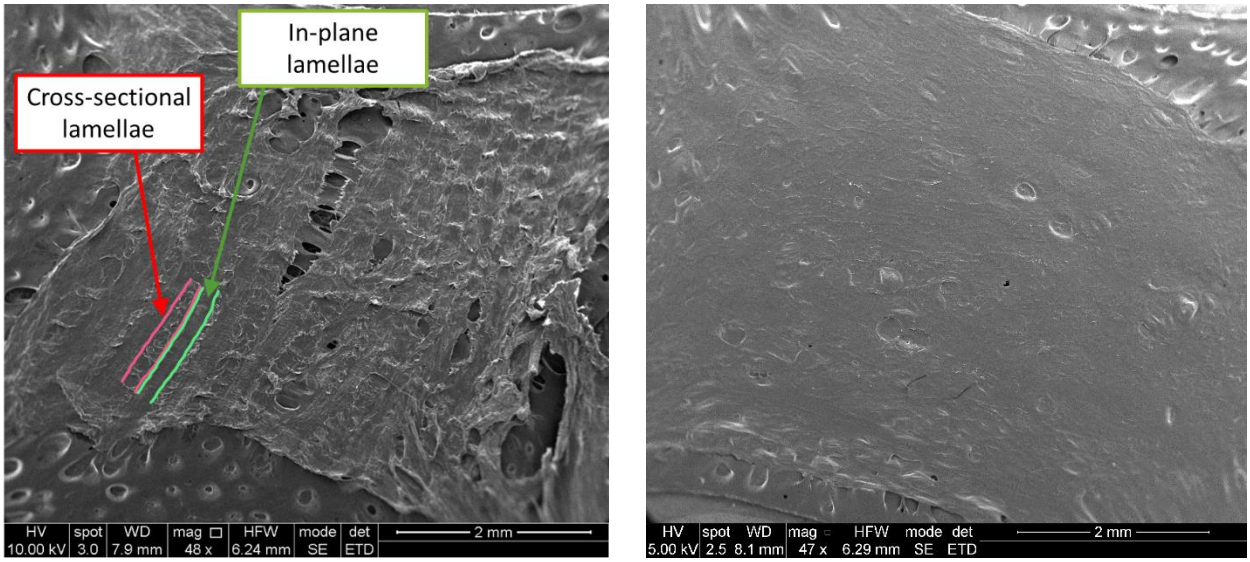

Figure 18. Lamellar sheet visibility comparison between sheep and human samples at a low magnification. Left: Sheep sample where cross-sectional and in-plane lamellae can be clearly seen. Right: Human sample where lamellar sheets cannot be as easily distinguished compared to sheep samples.

An unexpected result from the human sample experiment 1 (Table 1) was that increasing the sonication time did not necessarily increase the digestion of the sample (Figure 10). Since these samples were not obtained from adjacent samples (i.e. one sample could be from closer to the VEP compared to the other), it is likely that the samples were not identical in composition. Since digestion is not a homogenous process, some samples may be more susceptible to digestion than others based on their location in the AF. However, only the sample that was sonicated for 60 minutes had fenestrations where digestion had occurred and EF were visible (Figure 11).

After sonicating the samples for 60 minutes, digested areas appeared where only EF were present. Since sequential images were taken on the SEM zooming into the location where the EF were found, EF could be easily determined to be in the lamellae or ILM regions. EF in the human samples were located at the ILM-lamellae boundary based on the lamellar sheets visible on the surface of the sample (Figure 11). Based on the locations of the lamellar sheets and as found in sheep AF, EF were present in both the lamellae and the ILM region. EF of two sizes can be seen where some fibres were thicker while others were finer. Thicker fibres appeared to be connected together by thinner fibres creating a network structure similar to results described in previous studies (Figure 11). EF in human AF created a network structure that spanned the ILM region and merged into the lamellar sheets.

Due to the presence of undigested ECM that covered the EF at the ILM-lamellae boundary, the concentration of NaOH was increased. However, since the sonication time for digestion using 1.0M NaOH for human discs had not been previously reported, sonication was stopped at 30 minutes to prevent over-digestion. Over-digestion was observed during sonication where the samples broke into smaller pieces which removed components where the EF could anchor. Hot alkali digestion prior to sonication was too harsh resulting in samples that were smaller than originally prepared and did not have visible lamellar sheets (Figure 8). Soaking the samples in NaOH also resulted in samples that were over-digested. During the soaking process, the samples had become very susceptible to digestion and therefore when they were sonicated, the entire outer layer of the sample had digested. The appearance of an under-digested sample after the soaking process was misleading however based on the sample tears, it seems that the digestion process had begun on a lower level of the AF sample. In both cases of over-digestion, the ECM was removed too quickly and aggressively leading to damage to the EF network that lies underneath.

Sonication the human AF sample for 30 minutes in 1.0M NaOH, however, was not enough time for the sample to digest sufficiently (Figure 13). Sonication leads to the samples being digested from the outside to the inside and EF were, therefore, observed on the outer edge of the sample. In the obliquely cut sample, EF could be seen behind small holes indicating an area where digestion had begun but had not occurred for long enough to reveal the whole EF network underneath. The cutting angle did not have an obvious effect on the digestion process since both horizontally and obliquely cut samples showed evidence of digestion (Figure 12, Figure 13). Visualizing the lamellar sheets was more difficult with samples that were horizontally cut compared to obliquely cut samples.

Since the sample was horizontally cut, the lamellar sheets could be recognized by the change in the direction of the collagen bundles rather than the appearance of a textured surface as with obliquely cut samples. Although sequential images were taken, location of the EF could not be determined accurately since the EF were found at the very edge of the sample (Figure 12). EF were seen that were primarily parallel to each other and did not create a network. Undigested matrix created the appearance of a network structure on the right side of the SEM image in Figure 12. However, undigested matrix can be seen that obscured the EF, by creating a webbing between the EF mimicking a network structure. Without complete removal of the

ECM, the ultrastructure of the EF network cannot be accurately determined. A similar result was obtained in the samples that were sonicated for 120 minutes (Figure 16). Interestingly more ECM could be seen obscuring the EF network in the sample that was digested for 120 minutes. Location of the sample within the AF plays a role in the effectiveness of the partial alkali digestion process.

Due to the over-digestion that occurred in the samples that were soaked overnight in 1.0M NaOH, a slower process of digestion was undertaken. By sonicating the samples for a longer duration, the ECM could be removed gently therefore preserving the EF network underneath. In samples that were sonicated for 60 minutes and 90 minutes, EF networks were partially visible and appeared to have been torn. Tearing of the EF network could be a result of sample mishandling, over-digestion, or from the SEM. Sample mishandling resulted in torn samples using sheep AF samples, even when not using forceps. Over-digestion can lead to ECM removal that results in damage to the EF network and has been shown to occur non-homogenously in human AF samples. Another factor that may contribute to damage to the EF network is imaging using SEM.

The effect of SEM on the EF network had not been previously seen in this project. SEM is a process by which a focused electron beam is directed at the sample to produce signals that are processed into a high-resolution image. It was common knowledge from the beginning of this project that using a high voltage beam, although would result in a higher resolution image, could damage the sample. During the imaging process in the final experiment, an EF could be seen recoiling live as an effect of the electron beam. It is possible then that during the process of scanning the sample for digested areas that the electron beam had damaged the EF networks that had been exposed as a result of the digestion process. Therefore, for the rest of the imaging, the lowest voltage (2kV) was chosen to visualise the EF.

SEM imaging skills was another factor that contributed to the success of each experiment. With the skillset at the end of the project, the sheep AF sample that was digested at the beginning of the project could have yielded much more information about the EF network. Digested regions could be seen in the second attempt of sheep experiment 1 (Table 1) that were not further analysed during the SEM session because identifying locations where digestion had occurred was a skill that was learned throughout the course of the project. Evidence of the effect of SEM imaging was clear in that EF could only be found on the second

day of imaging the same samples from the same experiment. Imaging by SEM was a time-consuming process that was more effective when spanned across multiple days rather than one long session. This difference in effectiveness of SEM imaging is due to an increase in human error that would occur as a result of fatigue.

EF were primarily located at the edge of human AF samples which meant that it is unclear whether the EF were located in the lamellae or the ILM region. EF were hypothesized to play a role in maintaining the structural integrity of the AF by allowing it to return to its original shape after deformation (such as during compression). EF were located at the boundary between the lamellae and the ILM merging from the ILM into the lamellae. By merging into the lamellae, EF acts to hold adjacent lamellar sheets together to prevent it from separation during radial bulging, bending, and shear loading. EF are recruited during any motion that could cause the lamellae to separate. The ultrastructure of the EF was similar to that described in previous studies that described EF primarily parallel to each other in the lamellae and creating a mesh structure in the ILM (Tavakoli and Costi, 2017, Tavakoli et al., 2017). Undigested matrix obscured the EF network in many instances of locating EF in the human samples and made it difficult to obtain information on the size and organization of the EF.

Table 2. Summary of experiments conducted in this project rated for digestion from 1-6 from least digested to most digested sample (a rating of 4 is optimal).

Experiment	Experiment Description	Digestion Rating	Digestion Observations
Sheep Exp. 1	Sonicated for 25 minutes in 0.5M NaOH	4	Optimal digestion; digested areas clearly visible
Sheep Exp. 2	Hot alkali pre-sonication treatment	6	Over-digested; samples were damaged
Human Exp. 1	Sonicated for 15 minutes in 0.5M NaOH	2	Under-digested; fibrous components were visible in the sample but no EF or digested areas
Human Exp. 1	Sonication for 30 minutes in 0.5M NaOH	1	Under-digested; no fibrous components were visible in the sample or digested areas
Human Exp. 1	Sonicated for 60 minutes in 0.5M NaOH	3	Suboptimal digestion; EF could be found at the ILM-lamellae boundary, but not many digested areas were found
Human Exp. 2	Sonicated for 30 minutes in 1.0M NaOH	3	Suboptimal digestion; EF could only be found at the edge of the sample
Human Exp. 3	Overnight soak in 1.0M NaOH	6	Over-digestion; samples were damaged
Human Exp. 4	Sonicated for 60 or 90 minutes in 1.0M NaOH	5	Slightly over-digested; Partial EF networks were found
Human Exp. 4	Sonicated for 120 minutes in 1.0M NaOH	3	Slightly under-digested; EF networks were found at the edge of the sample that were obscured by ECM

Variations from the expected results were abundant. Increasing sonication time was expected to remove ECM, however, two instances of the opposite result was obtained during this project. Using 0.5M NaOH, samples sonicated for 15 minutes appeared to be more digested than the samples that were sonicated for 30 minutes. Then, when the sample was sonicated for 30 minutes using 1.0M, EF found at the edge of the sample were less obscured by ECM compared to EF found at the edge of a sample that was sonicated for 120 minutes. All experiments conducted and results are summarized in Table 2. A qualitative rating of digestion was given to all experiments from 1-6 from no digestion to over-digested. None of the optimization experiments resulted in an optimal digestion rating of 4, but slightly under-digested and slightly over-digested results were obtained (Table 2). EF ultrastructure was hypothesized to differ between regions of the disc, degeneration grade, and disc level. In order to minimize the effect of degeneration grade and disc level, the same L1/L2 disc was used to conduct all the human sample AF experiments since the upper lumbar levels experience less degeneration than lower levels. Differences in lamellae are apparent in

posterior regions compared to all other regions in the disc, therefore lateral and anterior regions were used. Inconsistent effect of sonication duration on the samples (i.e. longer sonication did not mean decreased ECM) could be indicative of differences in the concentrations of the constituents in the disc closer to the VEP. Experiments conducted changing sonication time should be repeated using different disc sample to determine cause of inconsistencies.

Future Work

Further experimentation is required to optimise the partial alkali digestion protocol for use in human AF samples to determine the differences in EF based on disc level, sample region, and degeneration. It is evident from the results in this study that a gentle procedure is required for the removal of the ECM to retain EF from the AF samples. Using a hot alkali pre-sonication treatment resulted in samples that were too damaged to be used for visualisation of the EF network. Although soaking the samples in 1.0M NaOH also led to sample damage, it may be beneficial to determine the effect of soaking the samples in NaOH of a lower concentration and for a shorter duration. However, testing efficacy of this potential methodology would require extensive experimentation to determine the concentration of NaOH, duration of the soak, and then duration of sonication (considering that sonication for 2 minutes resulted in samples that were over-digested). All samples that were used in this project were 30µm as the original protocol had used, but a thicker sample should be explored if a harsher digestion protocol is used.

In keeping with the theme of the experiments that were found to be successful in this project, sonication duration should be varied to successfully visualise EF. Results from human experiment 4 indicate that 1.0M NaOH led to samples that had retained ECM at the edges and did not have complete EF networks towards the centre of the sample. Instead of using 1.0M NaOH, initial experimenting should begin with reproducing human sample experiment 2 sonicating samples for 120 minutes and longer using 0.5M NaOH. Since ECM covers the EF network in the ILM (where they are most prominent and play the largest functional role), using 0.5M NaOH provides a gentle removal of ECM that would result in retaining the ultrastructure of the underlying EF. Harsh removal of the ECM could lead to damage to the EF network in the ILM region.

Since the lamellar sheets in human AF are more densely organized compared to sheep AF, the post-sonication hot water treatment duration may also need to be increased. Collagen removal is necessary for creating digested regions where the EF can be visualised in the ILM region due to its small size. In order to maintain consistency between the experiments, samples were placed in the hot water bath for 12 minutes. However, in the study that developed the partial alkali digestion, a range of 12-15 minutes was stated for the post-sonication hot water treatment in human AF samples (Tavakoli and Costi, 2017). A hot water

treatment of 15 minutes may have encouraged further removal of the collagen fibres to better visualise the EF.

Although sonication power is another factor that was considered for the effectiveness of the protocol in visualisation of EF in human AF, a higher frequency may cause sample damage that would hinder the visualisation of EF. Since most of the experiments found that the EF were obscured by ECM, it is unlikely that a lower sonication power would be beneficial. An optimised digestion protocol could be used to visualise the structure and organization of EF in different regions of the disc and discs of different levels of degeneration.

As mentioned previously in the Gaps Analysis section, micromechanical testing could be conducted on a digested AF sample containing isolated EF in order to determine the mechanical properties of EF. Previous studies have demonstrated the function of EF in the disc by removing EF by enzymatic treatment which found that separation of lamellae was more likely in the absence of EF. However, enzymatic treatments were unable to remove only the EF and therefore the results obtained could be as a result of removal of other components. It would be highly beneficial for the furthering the understanding of the structure and function of EF in human AF to optimise this partial alkali digestion protocol.

Conclusion

Visualisation of the EF network in human AF can provide further insight into the structure and function of EF in the human intervertebral discs. Previous studies have isolated EF networks by partial alkali digestion in sheep AF and have been visualised by SEM in high-resolution. Partial alkali digestion protocol was successfully replicated in this project and a sequence of experiments were conducted to optimise the visualisation of EF in human AF. EF were found in lamellae and ILM regions in human AF during optimization. Consistent with previous studies, EF in the ILM created a network structure of thicker fibres interconnected by thinner fibres that merged into the lamellae. In the lamellar regions, EF were found to be mostly parallel to each other. Structure of the EF suggests a functional role in maintaining the structural integrity of the intervertebral disc. EF are recruited during deformation of the disc and maintain connectivity between lamellae to prevent permanent deformation. Changes in the EF organization and structure can be seen in degenerated discs or discs that are more susceptible to herniation which presents the clinical relevance of understanding the functional role of EF in the discs.

An optimal level of digestion was not achieved in the results presented in this study. However, results indicated that digestion is likely to be optimised with further experimentation. A gentle sonication procedure was shown to be more successful in visualisation of EF. An optimal digestion protocol should be used to compare the EF structure and organization in different regions of the disc and between discs of different levels of degeneration. After optimal digestion protocol has been developed, micromechanical tests should be conducted on digested samples to determine the mechanical properties of the EF in the disc. Visualisation of the EF network can provide further insight into the mechanisms of disc degeneration and herniation.

Bibliography

ABS 2019. Microdata: National Health Survey, 2017-2018, Detailed Microdata, DataLab. *In:* STATISTICS, A. B. O. (ed.).

BACHMEIER, B. E., NERLICH, A., MITTERMAIER, N., WEILER, C., LUMENTA, C., WUERTZ, K. & BOOS, N. 2009. Matrix metalloproteinase expression levels suggest distinct enzyme roles during lumbar disc herniation and degeneration. *Eur Spine J,* 18**,** 1573-86.

BOGDUK, N. 2012. *Clinical and radiological anatomy of the lumbar spine,* Edinburgh ; New York, Churchill Livingstone.

BRASSART, B., FUCHS, P., HUET, E., ALIX, A. J., WALLACH, J., TAMBURRO, A. M., DELACOUX, F., HAYE, B., EMONARD, H., HORNEBECK, W. & DEBELLE, L. 2001. Conformational dependence of collagenase (matrix metalloproteinase-1) up-regulation by elastin peptides in cultured fibroblasts. *J Biol Chem,* 276**,** 5222-7.

CREAN, J. K., ROBERTS, S., JAFFRAY, D. C., EISENSTEIN, S. M. & DUANCE, V. C. 1997. Matrix metalloproteinases in the human intervertebral disc: role in disc degeneration and scoliosis. *Spine (Phila Pa 1976),* 22**,** 2877-84.

FAURY, G., USSON, Y., ROBERT-NICOUD, M., ROBERT, L. & VERDETTI, J. 1998. Nuclear and cytoplasmic free calcium level changes induced by elastin peptides in human endothelial cells. *Proc Natl Acad Sci U S A,* 95**,** 2967-72.

FAZZALARI, N. L., COSTI, J. J., HEARN, T. C., FRASER, R. D., VERNON-ROBERTS, B., HUTCHINSON, J., MANTHEY, B. A., PARKINSON, I. H. & SINCLAIR, C. 2001. Mechanical and pathologic consequences of induced concentric anular tears in an ovine model. *Spine (Phila Pa 1976),* 26**,** 2575-81.

GRANT, M. P., EPURE, L. M., BOKHARI, R., ROUGHLEY, P., ANTONIOU, J. & MWALE, F. 2016. Human cartilaginous endplate degeneration is induced by calcium and the extracellular calcium-sensing receptor in the intervertebral disc. *Eur Cell Mater,* 32**,** 137-51.

GREGORY, D. E., BAE, W. C., SAH, R. L. & MASUDA, K. 2012. Anular delamination strength of human lumbar intervertebral disc. *Eur Spine J,* 21**,** 1716-23.

GREGORY, D. E., BAE, W. C., SAH, R. L. & MASUDA, K. 2014. Disc degeneration reduces the delamination strength of the annulus fibrosus in the rabbit annular disc puncture model. *Spine J,* 14**,** 1265-71.

IATRIDIS, J. C., MACLEAN, J. J., O'BRIEN, M. & STOKES, I. A. 2007. Measurements of proteoglycan and water content distribution in human lumbar intervertebral discs. *Spine (Phila Pa 1976),* 32**,** 1493-7.

JUNG, S., RUTKA, J. T. & HINEK, A. 1998. Tropoelastin and elastin degradation products promote proliferation of human astrocytoma cell lines. *J Neuropathol Exp Neurol,* 57**,** 439-48.

LEE, S. H., DERBY, R., CHEN, Y., SEO, K. S. & KIM, M. J. 2004. In vitro measurement of pressure in intervertebral discs and annulus fibrosus with and without annular tears during discography. *Spine J,* 4**,** 614-8.

MECHAM, R. P., BROEKELMANN, T. J., FLISZAR, C. J., SHAPIRO, S. D., WELGUS, H. G. & SENIOR, R. M. 1997. Elastin degradation by matrix metalloproteinases. Cleavage site specificity and mechanisms of elastolysis. *J Biol Chem,* 272**,** 18071-6.

MIKAWA, Y., HAMAGAMI, H., SHIKATA, J. & YAMAMURO, T. 1986. Elastin in the human intervertebral disk. A histological and biochemical study comparing it with elastin in the human yellow ligament. *Arch Orthop Trauma Surg,* 105**,** 343-9.

PFIRRMANN, C. W., METZDORF, A., ZANETTI, M., HODLER, J. & BOOS, N. 2001. Magnetic resonance classification of lumbar intervertebral disc degeneration. *Spine (Phila Pa 1976),* 26**,** 1873-8.

SCHOLLUM, M. L., ROBERTSON, P. A. & BROOM, N. D. 2008. ISSLS prize winner: microstructure and mechanical disruption of the lumbar disc annulus: part I: a microscopic investigation of the translamellar bridging network. *Spine (Phila Pa 1976),* 33**,** 2702-10.

SMITH, L. J., BYERS, S., COSTI, J. J. & FAZZALARI, N. L. 2008. Elastic fibers enhance the mechanical integrity of the human lumbar anulus fibrosus in the radial direction. *Ann Biomed Eng,* 36**,** 214-23.

SMITH, L. J. & FAZZALARI, N. L. 2006. Regional variations in the density and arrangement of elastic fibres in the anulus fibrosus of the human lumbar disc. *J Anat,* 209**,** 359-67.

SMITH, L. J. & FAZZALARI, N. L. 2009. The elastic fibre network of the human lumbar anulus fibrosus: architecture, mechanical function and potential role in the progression of intervertebral disc degeneration. *Eur Spine J,* 18**,** 439-48.

TAVAKOLI, J., AMIN, D. B., FREEMAN, B. J. C. & COSTI, J. J. 2018. The Biomechanics of the Inter-Lamellar Matrix and the Lamellae During Progression to Lumbar Disc Herniation: Which is the Weakest Structure? *Ann Biomed Eng,* 46**,** 1280-1291.

TAVAKOLI, J. & COSTI, J. J. 2017. Development of a rapid matrix digestion technique for ultrastructural analysis of elastic fibers in the intervertebral disc. *J Mech Behav Biomed Mater,* 71**,** 175-183.

TAVAKOLI, J. & COSTI, J. J. 2018a. A method for visualization and isolation of elastic fibres in annulus fibrosus of the disc. *Mater Sci Eng C Mater Biol Appl,* 93**,** 299-304.

TAVAKOLI, J. & COSTI, J. J. 2018b. New findings confirm the viscoelastic behaviour of the inter-lamellar matrix of the disc annulus fibrosus in radial and circumferential directions of loading. *Acta Biomater,* 71**,** 411-419.

TAVAKOLI, J. & COSTI, J. J. 2018c. New insights into the viscoelastic and failure mechanical properties of the elastic fiber network of the inter-lamellar matrix in the annulus fibrosus of the disc. *Acta Biomater,* 77**,** 292-300.

TAVAKOLI, J. & COSTI, J. J. 2018d. Ultrastructural organization of elastic fibres in the partition boundaries of the annulus fibrosus within the intervertebral disc. *Acta Biomater,* 68**,** 67-77.

TAVAKOLI, J., ELLIOTT, D. M. & COSTI, J. J. 2016. Structure and mechanical function of the inter-lamellar matrix of the annulus fibrosus in the disc. *J Orthop Res,* 34**,** 1307-15.

TAVAKOLI, J., ELLIOTT, D. M. & COSTI, J. J. 2017. The ultra-structural organization of the elastic network in the intra- and inter-lamellar matrix of the intervertebral disc. *Acta Biomater,* 58**,** 269-277.

USHIKI, T. 2002. Collagen fibers, reticular fibers and elastic fibers. A comprehensive understanding from a morphological viewpoint. *Arch Histol Cytol,* 65**,** 109-26.

VERES, S. P., ROBERTSON, P. A. & BROOM, N. D. 2008. ISSLS prize winner: microstructure and mechanical disruption of the lumbar disc annulus: part II: how the annulus fails under hydrostatic pressure. *Spine (Phila Pa 1976),* 33**,** 2711-20.

VERES, S. P., ROBERTSON, P. A. & BROOM, N. D. 2009. The morphology of acute disc herniation: a clinically relevant model defining the role of flexion. *Spine (Phila Pa 1976),* 34**,** 2288-96.

VERES, S. P., ROBERTSON, P. A. & BROOM, N. D. 2010. The influence of torsion on disc herniation when combined with flexion. *Eur Spine J,* 19**,** 1468-78.

VERNON-ROBERTS, B., MOORE, R. J. & FRASER, R. D. 2007. The natural history of age-related disc degeneration: the pathology and sequelae of tears. *Spine (Phila Pa 1976),* 32**,** 2797-804.

YU, J. 2002. Elastic tissues of the intervertebral disc. *Biochem Soc Trans,* 30**,** 848-52.

YU, J., FAIRBANK, J. C., ROBERTS, S. & URBAN, J. P. 2005. The elastic fiber network of the anulus fibrosus of the normal and scoliotic human intervertebral disc. *Spine (Phila Pa 1976),* 30**,** 1815-20.

YU, J., TIRLAPUR, U., FAIRBANK, J., HANDFORD, P., ROBERTS, S., WINLOVE, C. P., CUI, Z. & URBAN, J. 2007. Microfibrils, elastin fibres and collagen fibres in the human intervertebral disc and bovine tail disc. *J Anat,* 210**,** 460-71.

YU, J., WINLOVE, P. C., ROBERTS, S. & URBAN, J. P. 2002. Elastic fibre organization in the intervertebral discs of the bovine tail. *J Anat,* 201**,** 465-75.

Appendices

Appendix A (Further Images of Sheep Experiments)

Sheep Sample Experiment 1 (Trial 1)

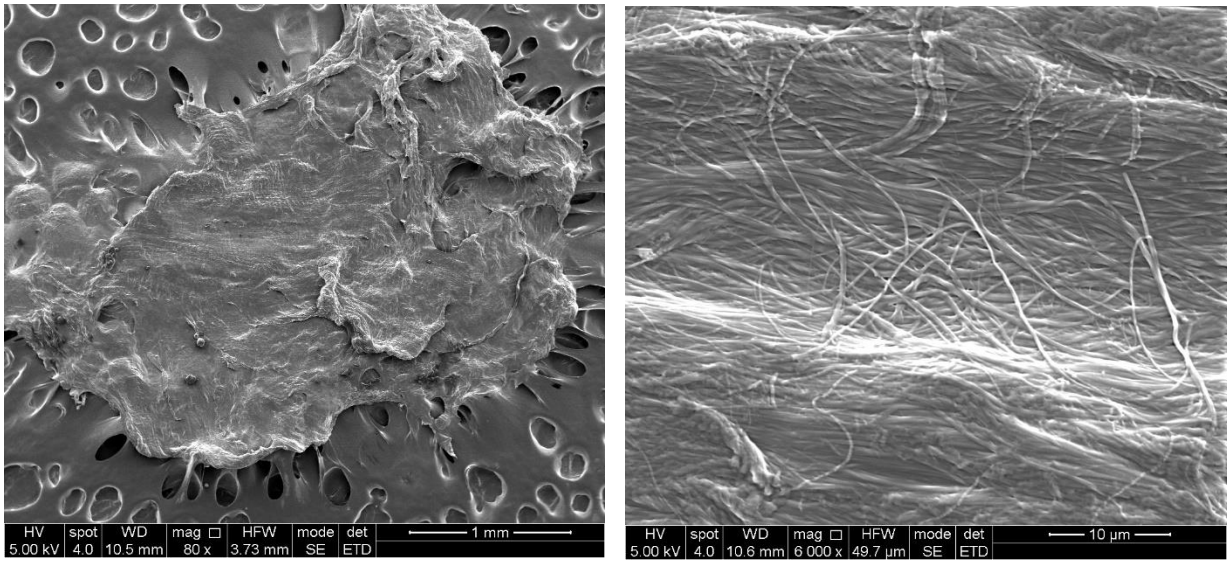

Figure 19. SEM images of sheep sample experiment 1 trial 1. Both images are from the same sample. Left: zoomed out image showing the sample with folds and unidentifiable structures. Right: unidentifiable fibres.

Sheep Sample Experiment 1 (Trial 2)

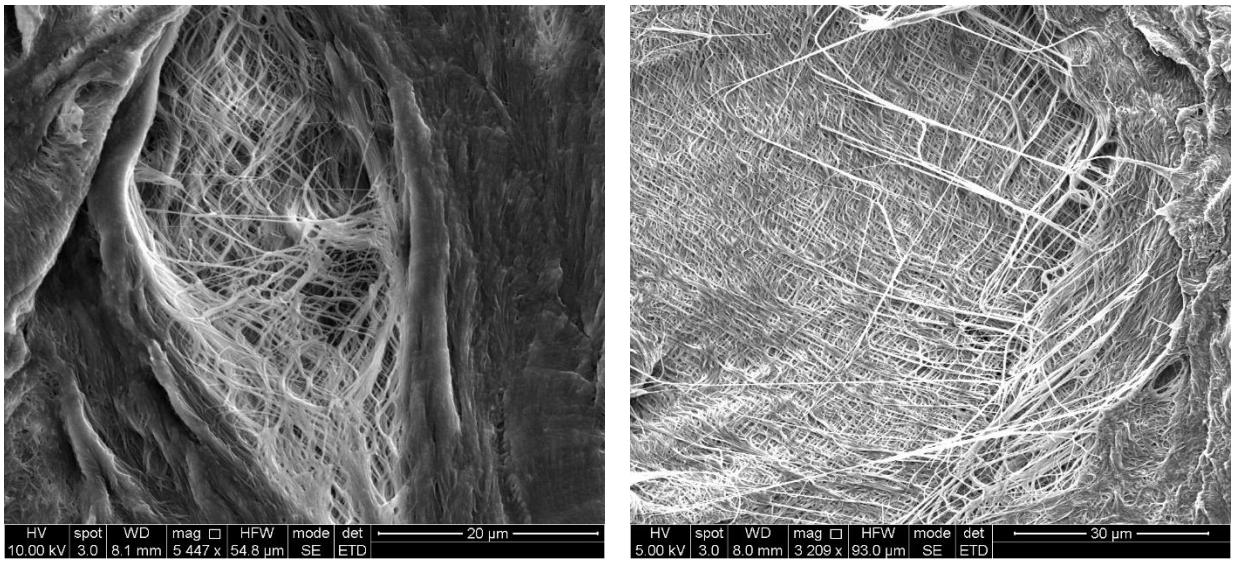

Figure 20. SEM images of sheep sample experiment 1 trial 2. Images are from different samples. EF can be seen of primarily the same size oriented in the same direction. Location of EF was likely within the lamellae.

Sheep Sample Experiment 2

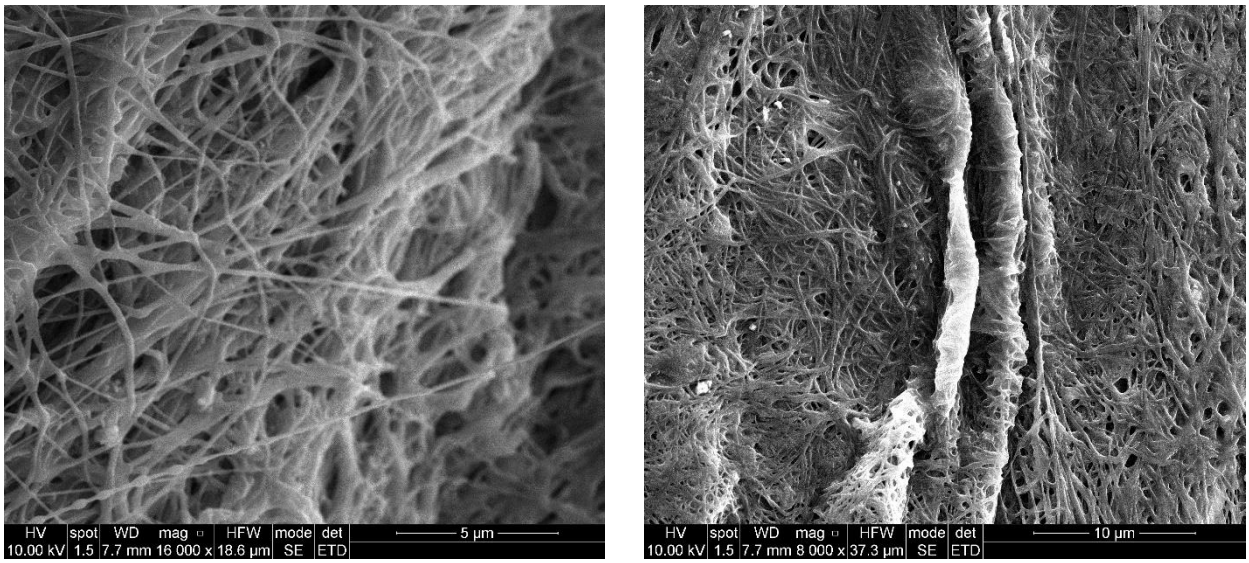

Figure 21. SEM images from Sheep sample experiment 2. Both images are from samples that were hot alkali digested for 2 minutes. Fibres can be clearly seen that were likely collagen based on their structure.

Appendix B (Further Images of Human Experiments)

Human Sample Experiment 1

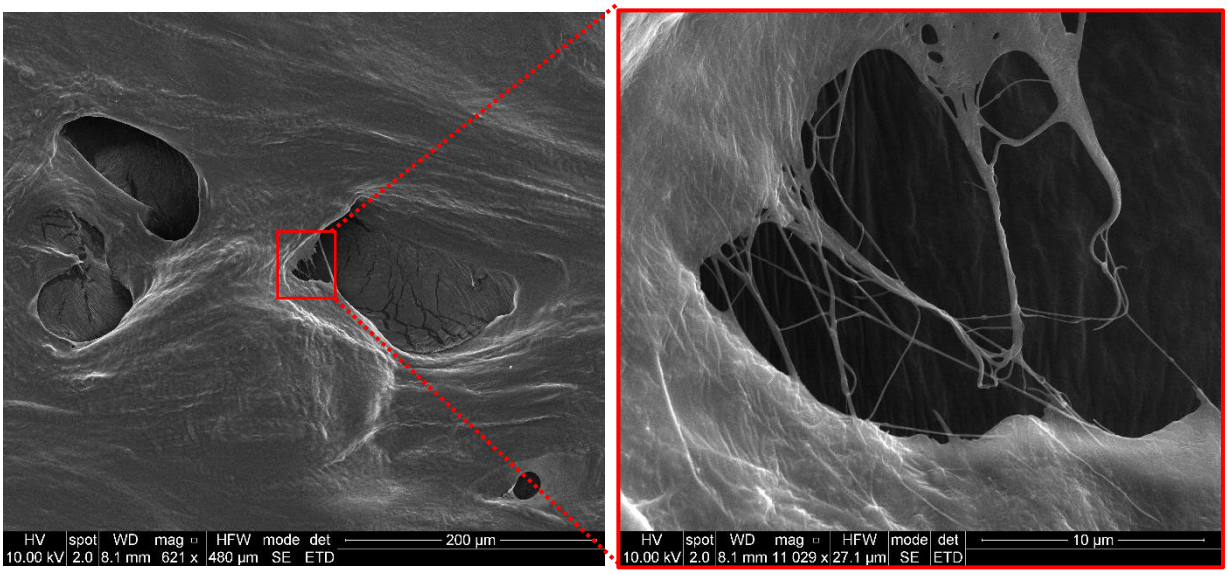

Figure 22. SEM images from human experiment 1 sonicated for 60 minutes. Both images are from the same sample. Left: zoomed out picture indicating location of EF as in within the lamellae. Right: EF can be seen oriented primarily parallel to each other.

Human Sample Experiment 2

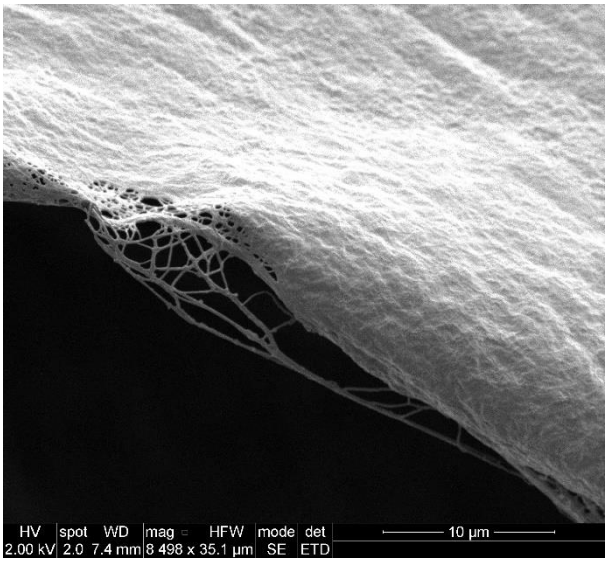

Figure 23. SEM image from human experiment 2. EF found at the edge of the sample indicating that digestion had begun.

Human Sample Experiment 3

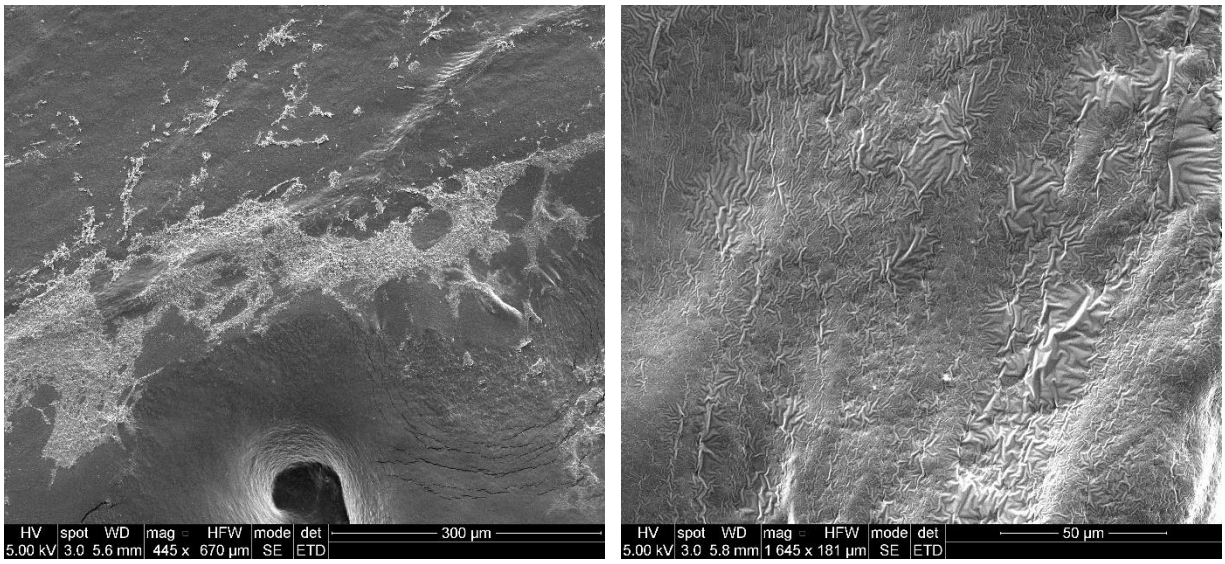

Figure 24. SEM images from human sample experiment 3. Both images are horizontally cut samples. Left: sample sonicated for 30 minutes. Debris from the sonication can be seen trapped in the sample. Right: sample sonicated for 60 minutes. Sonication appeared to have created a structure on the surface of the sample making EF hard to locate.

Human Sample Experiment 4

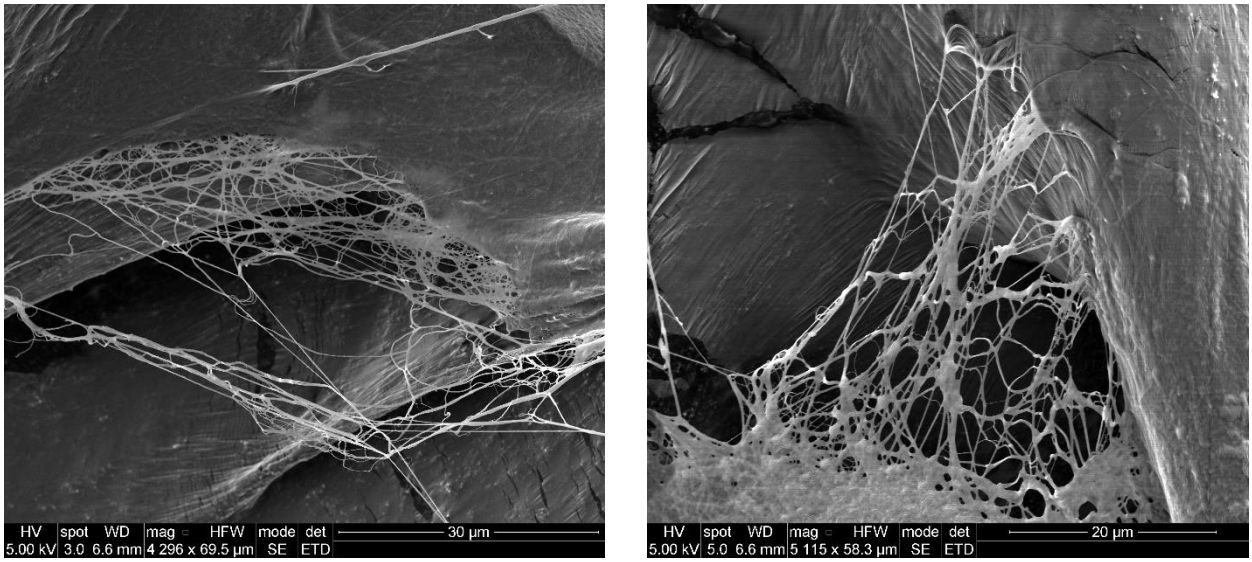

Figure 25. SEM images from human sample experiment 4. Both images are from samples that were sonicated for 60 minutes. EF can be seen of primarily the same size.